AN ABSTRACT OF THE THESIS OF

Wenxin Ke for the degree of Master of Science in Chemistry presented on February 23, 1998.

Title: **Supercooling and Kinetics of Freezing of Benzene Clusters as Studied by Coherent Anti-Stokes Raman Spectroscopy.**

Abstract approved: Redacted for Privacy

Joseph W. Nibler

Coherent Anti-Stokes Raman Spectroscopy (CARS) was used to study the supercooling and kinetics of freezing of benzene clusters formed in a supersonic jet. The CARS spectra show a Raman feature due to liquid drops of about 10 nm mean diameter. The temperature of the drop is deduced from the peak position, combined with a frequency-temperature relation determined for bulk samples examined in a cryostat. For colder expansions driven by helium, the temperature of the liquid cluster is observed to initially cool but then increase at large distances from the nozzle due to the onset of freezing. Direct conformation of this was not possible because the solid and liquid CARS peaks overlap at the supercooled nucleation temperature of 230 K. Nonetheless, the temperature rise is believed to be a positive indication that nucleation of freezing has occurred in about 0.36 μs and an upper limit of $J = 3.8 \times 10^{30}$ m^{-3} s^{-1} is obtained for the nucleation rate. From this and homogeneous nucleation theory a lower limit of $\sigma_{sl} = 11$ mJ m^{-2} is deduced for the liquid-solid surface free energy at 230 K.

Supercooling and Kinetics of Freezing of Benzene Clusters as Studied by Coherent Anti-Stokes Raman Spectroscopy.

by

Wenxin Ke

A THESIS

submitted to

Oregon State University

in partial fulfillment of
the requirements for the
degree of

Master of Science

Presented February 23, 1998
Commencement June 1998

Master of Science thesis of Wenxin Ke presented on February 23, 1998

APPROVED:

Redacted for Privacy

Major Professor, representing Chemistry

Redacted for Privacy

Chair of Department of Chemistry

Redacted for Privacy

Dean of Graduate School

I understand that my thesis will become part of the permanent collection of Oregon State University libraries. My signature below authorizes release of my thesis to any reader upon request.

Redacted for Privacy

Wenxin Ke, Author

Acknowledgment

If there is anything that I should feel proud of in my graduate studies at Oregon State University (OSU), it would be my appreciation of the logic of science through the influences of my mentor, Professor Joe W. Nibler. I thank him heartily for accepting me into his research group. I thank him for the training on research logic, skills and language. I would like to use an old Chinese saying "One day teacher, one's life time father". I really appreciate the time I spent with him at OSU.

I would like to thank Dr. John F. Ogilvie for his proof-reading of my thesis and informed discussion on issues of phase transitions and spectroscopy. I would also like to use this opportunity to express my appreciation to Dr. Thomas. I learned a great deal by working as his TA in P. Chem and had my desk in his lab in the first year.

I am very grateful to all the members of Dr. Nibler's group for their fellowship and assistance throughout these years on the first floor of Gilbert. I would like to thank Dr. Phil Minarik for teaching me lab skills when I first joined the group. I have also learned a great deal by watching and talking to the following people: Drs. Mansour Zahedi, Abdullah A. Al-Kahatani, Alan Richardson, Matthias Leuchs, Marshall Crew, Darren Williams, Michael Orlov, Steve Mayer, and Pooya Tadayon. I also enjoyed the time spent together with new members in the group, Engelene Chrysostom and Nicolae Vulpanovici. I thank them all for their kind help during my thesis work.

I am greatly indebted to my parents for their sacrifices to let their only child stay thousands of miles away to continue higher education. I am grateful to my beloved

fiancee, Nuria, for her encouragement and patience during the long run of my research and thesis writing.

TABLE OF CONTENTS

Page

1. INTRODUCTION 1

1.1 Kinetics of Phase Transitions 1

1.2 Solid-solid Phase Transitions of Benzene 6

1.2.1 Does benzene pre-melt ? 7
1.2.2 Does benzene have glass or other solid phases? 8

1.3 Summary 9

2. HOMOGENEOUS NUCLEATION THEORY FOR FREEZING 10

2.1 Introduction 10

2.2 Homogeneous Nucleation in a Gas 12

2.3 Homogeneous Nucleation Theory for Freezing 15

2.4 Approximate Relation for the Rate of Nucleation 19

2.5 Conclusion 21

3. EXPERIMENTAL DESIGN AND EXPERIMENTS 22

3.1 Basic Idea of Experiments 22

3.2 CARS System 22

3.2.1 Seeder technique for YAG laser 25
3.2.2 Bad shot detector 25

3.3 Sample System 26

3.3.1 Cryostat system for bulk sample 26
3.3.2 Molecular jet system for cluster.. 26

4. CARS STUDIES OF PHASE CHANGES IN EQUILIBRIUM BENZENE 30

4.1 Introduction 30

4.2. Experiments and Results 35

4.2.1 Apparatus and sample handling 35
4.2.2 Spectra and results 36
4.2.3 Analysis 39

TABLE OF CONTENTS (Continued)

4.3. Discussion 44

4.3.1 Solid-liquid phase change 44
4.3.2 Glass phase change 47
4.3.3 Other proposed solid phase changes 47
4.3.4 Existence of a premelting process 48

4.4 Conclusions 50

5. CARS STUDIES OF BENZENE CLUSTERS FORMED IN JET EXPANSIONS ... 51

5.1 Introduction 51

5.2 Experiments 53

5.2.1 Molecular free jet cooling mechanism 53
5.2.2 Free jet experiments with benzene 55
5.2.3 Determination of cluster temperature by Raman shift 55

5.3. Results and Analysis 57

5.3.1 Pure benzene vapor in a jet 57
5.3.2 Helium driven benzene for a large nozzle 62
5.3.3 Helium driven benzene in a small nozzle 67
5.3.4 Reliability of Raman shift measurements determined by CARS 74

5.4 Model of Supercooling and Freezing Processes 74

5.5. Determination of Interfacial Tension σ_{sl} of Solid from Jet Experiments 78

5.5.1 Introduction 78
5.5.2 Estimate of the mean size of clusters in the jet 79
5.5.3 Determination of the rate of nucleation 81
5.5.4 Determination of temperature of freezing 82
5.5.5 Determination of other physical parameters in equation (2.8) 82
5.5.6 Determination of σ_{sl} and estimate of uncertainty 82
5.5.7 Discussion 84

5.6 Summary 87

Bibliography 89

LIST OF FIGURES

Figure — Page

2-1 Gibbs free energy versus size of nucleus for two saturation ratios....14

2-2 Simulation of rate of nucleation for benzene from classical nucleation theory, equation (2.8)....17

2-3 Completion of solid fraction Fs versus Jvt....21

3-1 CARS experiment set-up for this thesis research....24

3-2 Sample cell used in cryostat for bulk benzene....27

3-3 Molecular jet....27

4-1 Structure of solid benzene[40]....31

4-2 Raman spectra of lattice mode near melting point[71]....33

4-3 CARS spectra of benzene in a cryostat for a cool-down sequence. The vapor spectrum was recorded in a separate cell....37

4-4 CARS spectra of benzene in a cryostat for a warm-up sequence. The vapor and liquid spectra are the same as in figure 4-3....38

4-5 Raman shifts of warm-up and cool-down sequence. Triangles are warm-up data, squares are cool-down data....41

4-6 Linewidth of CARS peaks of warm-up and cool-down process. Triangles are warm-up data, squares are cool-down data....42

4-7 Intensity of CARS peaks of warm-up and cool-down sequence. Triangles are warm-up data, squares are cool-down data....43

4-8 Raman shift versus temperature relation for bulk phases of benzene....46

5-1 CARS spectra of pure benzene vapor in jet expansions with the large nozzle. The benzene was at room temperature where it has a vapor pressure 82 torr. The nozzle temperature was at around 42 C....59

LIST OF FIGURES (Continued)

Figure — Page

5-2 CARS spectra of neat benzene vapor in jet expansions with the small nozzle. (D =0.5 mm). The benzene was at 62 C where it has a vapor pressure of 416 torr. The nozzle temperature was at 65 C.....60

5-3 CARS spectra of benzene in jet expansions with the large nozzle. The circles are experimental data, the solid lines are peakfitting curves. The benzene was at room temperature where it has a vapor pressure 82 torr. The helium driving pressure was at 3.4 atm. The mole ratio of benzene is 3.2%. The nozzle was at 42 C 63

5-4 CARS spectra of benzene in jet expansion with the large nozzle. The circles are experimental data, the solid lines are peak fitting curves. The benzene was at 295 K where it has a vapor pressure of 82 torr. The helium driving pressure was at 4.7 atm. The mole ratio of benzene is 2.3% . The nozzle was at 42 C 64

5-5 Raman shift of clusters in the large nozzle jet expansion. The benzene was at 295 k where it has a vapor pressure of 82 torr. The helium driving pressures were 3.4 or 4.7 atm, corresponding to mole ratios of 3.2% or 2.3%. The nozzle was at 42 C.....66

5-6 CARS spectra of benzene in jet expansion of Sept. 6, 1995. The helium driving pressure was 4.4 atm and the benzene was at 295 K. The benzene mole ratio is 2.5 %. The nozzle was at 42 C.....68

5-7 Raman shift versus X/D in the small nozzle (D=0.25 mm) jet expansion. Sept 6, 1995 data.....69

5-8 CARS spectra of benzene driven with 3.4 atm helium in the small nozzle jet. The nozzle temperature was around 42 C. The benzene mole ratio is 3.2%.....70

5-9 CARS spectra of benzene driven with 4.7 atm helium in the small nozzle jet. The nozzle temperature was around 42 C. The benzene mole ratio is 2.3%.....71

5-10 Raman shift of benzene clusters in the jet versus helium driving pressure.....72

5-11 Raman shift of benzene clusters in the jet with the small nozzle (May 21, 1996 data).....72

5-12 Model of spectral changes expected for freezing process.....76

LIST OF TABLES

Table		Page
4-1	Summary of spectrum calibration data of CO_2 and benzene vapor	40
4-2	Summary of Raman shift, width, and intensity of bulk benzene sample	45
5-1	Jet experiment of neat benzene vapor at room temperature for a large nozzle. June 23, 1996 data	61
5-2	Jet experiment of neat benzene vapor at 62 C for a small nozzle. May 22 1996 data	61
5-3	Helium driven benzene in a large nozzle. June 23, 1996 data	65
5-4	Sept 6,1995 jet experiment data summary.	75
5-5	May 21,1996 jet experiment data summary	75
5-6	Summary of all relevant parameters in equation (2.8)	83
5-7	Changes of surface tension versus temperature (T) or mean size of clusters diameter (D)	85
5-8	σ_{sl} Values from different methods	87

SUPERCOOLING AND KINETICS OF FREEZING OF BENZENE CLUSTERS AS STUDIED BY COHERENT ANTI - STOKES RAMAN SPECTROSCOPY

1. INTRODUCTION

Phase changes have been recognized and a source of wonder since ancient times. They are commonplace and simple in comparison with many of the chemical transformations studied by chemists. Freezing, the phase transition of liquid into solid, is not only important in daily life and industry, but modeling of this process is also useful in understanding the kinetics of the nucleation of all phase transitions. Despite this, a recent perspective in the journal Science[1] lamented our lack of understanding of the details of this freezing event. This thesis is an effort to add to this understanding, via a study of the kinetics of the nucleation process in the freezing of liquid benzene.

1.1. Kinetics of Phase Transitions

Although the thermodynamic description of phase changes has been well developed for a century,[2] the kinetic aspects have been troublesome to study. The kinetic process is an important factor needed for the simulation of material properties.[3,4] The kinetics of nucleation is the key to understanding the freezing process. Nucleation of freezing is the creation in a liquid of a small seed crystal which has sufficient stability that further growth is energetically feasible. Nuclei below a critical size are unstable because the surface energy is too high, as discussed later. When only one pure component is involved in nucleation, it is called homogeneous nucleation. When

another component, like an impurity, plays a role in the nucleation, the impurities catalyze the nucleation, and the process is called heterogeneous nucleation. Container surfaces can also trigger the nucleation event. Heterogeneous nucleation is the common cause of phase change in nature because most materials contain impurities and these impurities or container surfaces always have a big influence on nucleation.[5,6] However, for theoretical considerations, homogeneous nucleation is desirable for understanding the initiation of a phase change. It offers the simplest situation for which we can construct a physical model that can be tested with experiments.[7,8] Homogeneous nucleation theory is well developed[9], and it will be discussed in detail in chapter 2.

The technique of misting, breaking liquid into small drops (clusters), is the main method of achieving homogeneous nucleation experimentally.[9,10] Turnbull pioneered the use of this technique to study metal clusters and found that when metal is coated with organic solvent, it can be broken into drops of about 50 μm diameter. As they cooled, it was found that the metal clusters remained in the liquid state at the melting point (T_m) of bulk material, cooled further, and then froze at a temperature lower than T_m. This phenomenon is called supercooling. By monitoring the duration of the freezing process, the rate of nucleation was deduced. The data were used to compare with rates calculated from classical homogeneous nucleation theory. Using this method, Turnbull was able to determine the surface tension (σ_{sl}) of the liquid-solid interface, a key property which is very difficult to measure accurately by any other method. From his measurements for a number of materials, mostly metal and a few organic molecules, Turnbell deduced an empirical relation between surface tension and heat of fusion, given by

$$\sigma_{sl} = K \Delta H_{fus} / (V^2 N_a)^{1/3} \qquad (1.1)$$

In this equation, ΔH_{fus} is the heat of fusion at the melting point, V is the molar volume, N_a is the Avogadro constant and K is an empirical constant found to have a value of about 0.45 for metals and 0.32 for molecules.

Turnbull's method was clever, but left a question as to whether the assumption of homogeneous nucleation was correct. In particular, the organic coating might function as an impurity and thus heterogeneous nucleation at the surface could have occurred instead of homogeneous nucleation. In a subsequent study, Staveley[10] tried to avoid this potential problem by spraying very small liquid drops of molecules into a pre-chilled cloud chamber. In studying two dozen systems, he found that all molecules experienced supercooling and most of them froze into solid in a narrow range of temperature. Light scattering was used to monitor the onset of freezing. The duration of freezing was measured and from this the rate of nucleation was deduced. The interfacial surface tension of liquid-solid measured from his experiments was found to follow Turnbull's empirical relation, assuming the constant K = 0.32. The cloud chamber method used by Staveley does not introduce any added material other than hydrogen as chilling gas, thus the homogeneous condition is better approached. However, light scattering does not measure the duration of freezing very well, as the ability to distinguish liquid and solid clusters is not very sharp. In general, the measurements tend to overestimate the duration of the freezing process, resulting a lower rate of nucleation value than real freezing process.

A third method of determining σ_{sl} evolved as the supersonic jet expansion technique became a popular method to study small clusters of atoms and molecules, and some scientists started to study large clusters formed in jets.[11-14] Clusters containing hundreds to millions of molecules can be produced in a supersonic jet, resulting in a size diameter range of 5 to 50 nm. For clusters of more than 1000 units, it was discovered that their properties are essentially those of bulk materials.[13,15,16] In a series of studies, L.S. Bartell[17,18]and coworkers used electron diffraction to determine the phase of such large aggregates of molecules. These clusters were found to freeze, and, in a few cases, even undergo a phase transition from one solid phase to another in a jet. The size of cluster in these experiments was of the order of 10 nm in diameter, which is three orders of magnitude smaller than the drops formed in Turnbull and Staveley's experiments. The influence of trace impurities is much reduced for such small drops and, with pure ammonia gas, truly homogeneous nucleation conditions were claimed in Bartell's experiment.[19]

Spectroscopy is an alternative choice to study phase transitions in a jet. Although sensitive, infrared absorption methods[20-22] do not allow fine point-probing in the jet, as needed to observe phase changes. Electronic fluorescence experiments do have this capability but liquid-solid phases are not well distinguished.[23-26] However, Coherent anti-Stokes Raman Spectroscopy (CARS) can be successfully used to study phase transition of large clusters in jets, as shown in our laboratory and others.[13,14,27] Because the non-linear signal is only generated at the focus of the laser beams, CARS has excellent spatial resolution. Laser beams can be focused to a diameter of 0.1 mm and the speed of clusters in the jet is about 1000 m/s, which corresponds to nanosecond

time resolution in measuring the nucleation rates. This is much better spatial and temporal resolution than that of electron diffraction. CARS has also great spectral resolution and good sensitivity, features that make it the ideal tool to study phase transitions of large clusters formed in a jet.

Using either electronic diffraction or CARS spectroscopy to probe the liquid-solid phase transition, accurate rates of freezing can be obtained. If we assume these are determined by rate of formation of critical nuclei and use homogeneous nucleation theory,[9] the hard-to-measure surface tension between liquid and solid σ_{sl} can be calculated. For example, from electronic diffraction, L.S. Bartell[19] determined the interfacial free energy σ_{sl} for ammonia between liquid and solid phase to be 23 mJ m^{-2} at a supercooled liquid freezing temperature of 128 K. Using CARS as a probe, P. Minarik[28] determined σ_{sl} for acetylene to be 10.1 mJ m^{-2} at a supercooled freezing temperature of 155 K. Only a few other values exist in the literature. If σ_{sl} for more molecules could be measured by these same methods, a comparison of σ_{sl} among different molecules could lead to a better understand of homogeneous nucleation and properties of surface.

The criterion used to distinguish liquid from solid in acetylene clusters by CARS was the appearance of resolved spectral peaks for liquid and solid phases.[13,14] Unfortunately, in my efforts to apply the CARS method to other molecules, I found that line broadening of the spectra in the jet is a typical occurrence, so that small liquid-solid spectral shifts are not so easily resolved as in equilibrium samples.[29-31] In addition, for many molecules investigated, even when liquid-solid peaks are resolved in spectra of

bulk phases, they can become overlapped in a jet due to shifts caused by supercooling of the liquid clusters. This is a common event, resulting in the observation that liquid is hard to distinguish from solid for many molecules we investigated in the jet.

In this thesis, a less obvious indicator for the phase transition of freezing is utilized. For any supercooled liquid at a low temperature (T_L) that freezes into a solid, the solid rapidly warms to the melting point (T_m). The difference between T_m and T_L can be large in a jet because the aggregate typically experiences severe supercooling.[13,14,19,32] A temperature rise can thus serve to indicate the onset of freezing. In our work we show that small variations of Raman peak center positions due to such a temperature rise can be detected with CARS, and benzene was used to demonstrate experimentally that measurement of such shifts is feasible. The advantages and limitations of this approach will be discussed. A useful expression for the rate of freezing is derived and, with some assumptions, is used to measure the rate of nucleation from experiment without the need to have resolvable spectra between liquid and solid in the jet. Using this rate, the surface tension between liquid and solid of benzene is calculated from classical nucleation theory.[9,19]

1.2. Solid-solid Phase Transitions of Benzene

Most molecules have one or more solid phases and although no phase change has been definitely confirmed for solid benzene as it is cooled, there are a few suggestions of other structural changes as the solid is cooled. As discussed below, these involve pre-melting near the melting point T_m, glass phase formation around 220 to 230

K, an indication of molecular reorientation in the solid around 240 and 120 K, and a possible further phase change around 100 K. Whether any of these are real is uncertain and seeking evidence for them was a secondary motivation of our CARS measurements on equilibrium sample of benzene.

1.2.1. Does benzene pre-melt ?

In the process of melting, the structure of a solid collapses into the randomly oriented molecular structure of the liquid. Most simple molecules are believed to have only first-order phase transitions when they melt. The theory of first-order phase transitions predicts that such a transition as melting is rapid, with no pre-transitional effects, such as pre-melting. Pre-melting implies that the structure of the solid phase becomes partially modified towards that of the liquid phase as a sample approaches the melting point. For example, some long chain molecules with methyl groups on the end undergo a pre-melting step involving rotation of the end molecular groups prior to true melting, in which the actual lattice structure is lost. Such pre-melting is a second order phase transition.[33,34]

Some experimental results have suggested that pre-melting might occur for benzene. A powder diffraction x-ray study of the lattice parameters as a function of temperature close to the melting point showed large changes in the relative intensities of several diffraction peaks as the melting point was approached. It also showed a very large expansivity of the lattice **c** parameter and of the cell volume,[35]evidence claimed to indicate a pre-melting effect. Further support came from Raman spectra, which

displayed a marked decrease in frequency of the lattice modes at temperatures close to the melting point.[36,37] A similar drop with temperatures was also observed at non-ambient pressures.[38] Some additional support for the concept of pre-melting comes from measurements of the bulk thermal expansivity α_v for a number of molecular crystals; these studies as a function of pressure show a power law divergence of α_v as these crystals approach the melting transition.[39]

On the other hand, a neutron powder diffraction study[40] failed to see the pre-melting effects reported in the x-ray study. It was argued that the effects in x-ray were due to the formation of large crystalline samples and that the experiment was not suited to study this question. Further arguments involving the effect of impurities and the difficulties of working near the melting point have prevented the acceptance of the idea of pre-melting for benzene and for other small molecules.

1.2.2. Does benzene have glass or other solid phases?

Many molecules have a glass phase and it has been suggested that benzene has such a phase.[41] The evidence is line broadening seen in IR absorption spectra which suggests that a glass phase forms around 223 K.[42] At low temperature, NMR measurements have been interpreted in terms of a molecular reorientation about the sixfold symmetry axis occuring at 120 K,[41] and other work suggests that there may be an additional phase transition around 100 K.[40] None of these possibilities is supported by x-ray or neutron diffraction data, which indicates that the structure of solid benzene at all temperatures is orthorhombic.[40,43,44] Given these conflicting reports, we have

looked to see if any evidence for such phase transitions might be seen in our CARS spectra of solid benzene formed in a cryostat.

1.3. Summary

Benzene is examined by CARS in this thesis work. High resolution vibrational spectra of equilibrium liquid and solid samples were recorded from 8 K to 298 K and evidence for suggested solid-solid phase transitions was sought. This data was also used in jet studies of freezing of benzene clusters and the results were combined with homogeneous nucleation theory to determine σ_{sl}, the solid-liquid interfacial free energy of benzene.

2. HOMOGENEOUS NUCLEATION THEORY FOR FREEZING

Homogeneous nucleation theory applied to the freezing process is used in this study of kinetics of freezing for measurement of interfacial free energy between liquid and solid phases. Accordingly, some background theory is presented; more details are given in Turnbull's work.[9,45] Our application of this theory, with some assumptions, allows use of the experimental data obtained for benzene to deduce σ_{sl}, the interfacial free energy between liquid and solid.

2.1. Introduction

Classical homogeneous nucleation theory for a phase change dates back to 1876 and was first proposed by Gibbs.[46] The gas to liquid transition was examined because the easy measurement of the interfacial free energy (surface tension σ_{lv}) between vapor and liquid was useful in verifying the correctness of the theory. This theory (sometimes called the capillary model) proved quite successful for describing the vapor to liquid phase transition,[47,48] and it was then extended to nucleation in liquid to solid, and solid to solid phase transitions. However, because there was no easy direct way to measure the interfacial free energy σ_{sl} between a liquid and a solid, the theory was relatively untested. In the late 40's, Turnbull[49] advanced an experimental method for determining σ_{sl}, based on the assumption that the capillary model for a rate of phase transition applies to the freezing transition too. The interfacial free energy was derived from the

theory via an experimental measurement of the rate of nucleation of freezing. The surface tension between liquid and solid for metal and a few organic molecules was determined, and an empirical equation relating this to molecular properties was proposed.[9,45,49] However, as the method assumed no heterogeneous nucleation, a condition which is difficult to verify, further development of the theory and experiment was limited. This concern was greatly reduced with the introduction of supersonic techniques, which produce many small liquid clusters so that any impurities were dispersed. In addition, there was no container surface to trigger a phase change. In recent years, L.S. Bartell[6,50] has used electronic diffraction and our group at OSU has[13,14] used Raman spectroscopy to investigate the nucleation of the phase transition of freezing in a molecular jet. It has been found that clusters of more than about 1000 units can serve as a realistic model of bulk systems for the study of nucleation in phase transitions. The thesis work described here is an extension of this research on homogeneous nucleation.

We mention briefly that the formation of a critical nucleus can also be studied theoretically, using an explicit representation of the intermolecular potential energy surface function which characterizes an ensemble of molecules. The most common approaches are "molecular dynamics"[51] and "Monte Carlo"[52] calculations. In the "molecular dynamics" method, one calculates the trajectories of individual members of a small collection of molecules as the molecules undergo chaotic collisions, and looks for dense regions corresponding to nuclei that then grow. Commonly the systems comprise a few dozen to a few hundred molecules. The "Monte Carlo" method examines similar size and types of molecular systems but is not based on generating a

thermal distribution by random collisions. Instead, random molecules are moved through random displacements by some prescription, and the movement is accepted or rejected according to a preset criterion. Both methods have been applied in explanation of experiments of nucleation of freezing in supersonic jets as detected with electronic diffraction.[6,50] Further details about these statistical models are reviewed in reference.[51]

Other approaches to the theoretical treatment of nucleation of freezing are the "density functional theory"[53] and "partition functions from an approximate quantum mechanical model".[54] The density functional theory demonstrates considerable promise but has not yet been implemented into treatments suitable for routine analysis of experimental data. The theory's future improvement requires additional structural data for supercooled liquids, information which is currently not available.

2.2. Homogeneous Nucleation in a Gas

When a gas is cooled in the absence of nucleating catalysts, it will sustain a substantial super-saturation before embryos of the condensed phase appear. The nucleation process in such a gas takes place via the random growth of minute condensed aggregates or clusters of the vapor phase molecules. The transformation of a phase begins in a tiny region and spreads. When the amount of the new phase is very small, the surface energy contributes an important fraction to the energy of the small region.

In the homogeneous nucleation of condensation, the formation of an embryo droplet, assumed spherical, with a surface free energy proportional to its surface area produces an equilibrium vapor pressure higher than that of bulk. As the embryo is

formed from the vapor, its surface free energy increases from 0 to $4\pi r^2\sigma_{lv}$, where σ_{lv} is the surface free energy or surface tension between liquid and vapor phases per unit area, that is $\Delta Gs = 4\pi r^2\sigma_{lv}$. The free-energy changes due to volume change is $\Delta Gv = -(kT/v_m) \ln(p/p_0)$, where p is vapor pressure, p_0 is saturated vapor pressure of liquid, and v_m is the molecular volume. The total elevation of the free energy of an embryo droplet above that of a plane surface of pure sample is therefore

$$\Delta G = 4\pi r^2\sigma_{lv} - (4/3)\,\pi r^3 (k T/v_m) (\ln p/p_0) \qquad (2.1)$$

The significance of this expression is seen by plotting ΔG against r for a given value of $S = p/p_0$ at constant temperature, as in Figure 2-1. This curve displays a free-energy barrier for the growth of embryos at a given super-saturation. The free-energy level must be at least as high as the peak, characterized by the critical radius r*, for the embryo to grow. The critical radius r* is obtained by differentiating equation (2.1) and evaluating r at the maximum to give

$$r^* = 2\sigma_{lv} v_m / (k T \ln p/p_0) \qquad (2.2)$$

Once the super saturation is reached, the rate of the formation of liquid drops in a vapor is usually governed by the rate of nucleation (J) and not by transport in vapor. An Arrhenius type rate-law expression for J is assumed to apply to the gas-liquid phase transition,

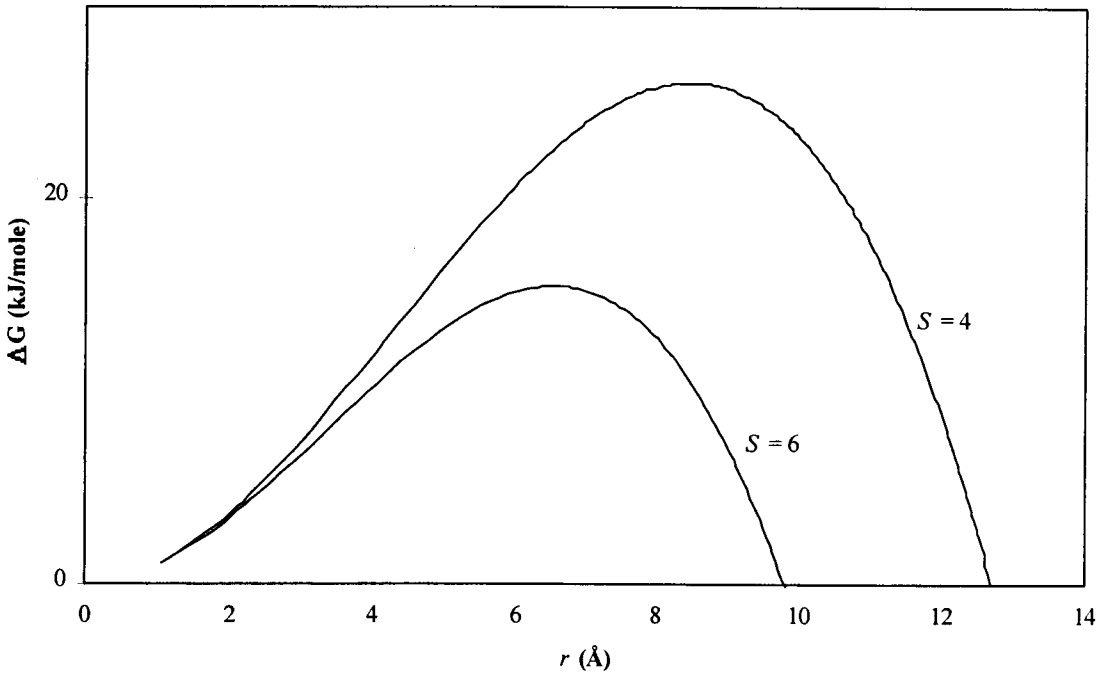

Figure 2-1. Gibbs free energy versus size of nucleus for two saturation ratios.

$$J = A \, Exp \, (\Delta G^* / k \, T) \qquad (2.3)$$

where A is a prefactor contribution, determined by the surface area of the critical nucleus and the collision frequency per square centimeter second from the kinetic theory of gases. ΔG^* is the minimum Gibbs free energy that the nucleus needs to form a critical nucleus. These quantities can be expressed as[55]

$$A = \frac{4\,\pi\,p}{r^{*2}} \frac{1}{\sqrt{2\,\pi\,m\,k\,T}} \tag{2.4}$$

$$\Delta G^{*} = -16\pi\,\sigma_{lv}{}^{3} / 3[(kT / v_m)(\ln(p / p_0))]^2 \tag{2.5}$$

J is seen to be very sensitive to the value of σ_{lg}, a quantity that is relatively simple to obtain experimentally from capillary rise measurements. The good agreement between J from theory and experiments in early work was used to justify extension of the theory to more complicated transformations in condensed phases, such as the liquid to solid phase transition.

2.3. Homogeneous Nucleation Theory for Freezing

An extension of classical homogeneous nucleation theory from the condensing to freezing process is presented in detail in, for example, reference[9,45] and gives a means to predict with useful accuracy a rate of nucleation. The key result is that the rate of nucleation J, following Bartell's notation,[19] is :

$$J = [2(\sigma_{sl}k_bT)^{1/2}/(v_m{}^{5/3}\eta)]\,\exp(-\Delta G^{*} / k_bT) \tag{2.6}$$

in which σ_{sl} is surface tension, v_m is molecular volume, η is viscosity, k_b is the Boltzmann constant, and T is the temperature at which nucleation of the phase transition happens. The Gibbs energy barrier ΔG^{*} is $\Delta G^{*}=16\pi\sigma_{sl}{}^{3}/(3\Delta G_v{}^{2})$, in which $\Delta G_v(T)$ is the Gibbs energy of the phase transition defined according to

$$\Delta G_v(T) = -(1/V)\int_{T}^{T_m} \Delta S_{fus}(T)dT \qquad (2.7)$$

in which $\Delta S_{fus}(T)$ is the entropy change of phase transition, and V is the molar volume. Substituting ΔG^* into equation (2.6), we have

$$J = [2(\sigma_{sl}k_bT)^{1/2}/(v_m^{5/3}\eta)] \exp(-16\pi\sigma_{sl}^3/(3\Delta G_v^2)k_bT) \qquad (2.8)$$

The pre-exponential factor (which we term A) of equation (2.8) describes the movement of molecules to the nucleation surface for the phase change. It decreases as the temperature decreases; a simulation using reasonable parameters for benzene (Figure 2-2) shows that this significantly affects the rate of nucleation when the temperature is less than 130 K. The exponential part describes the barrier that the liquid must overcome to freeze; the simulation shows that the value of the exponential part decreases rapidly for temperatures greater than 230 K. Overall, the model shows that the rate of nucleation J initially increases rapidly as temperature decreases, but then is nearly constant with temperature over a wide range. J is very sensitive to the value chosen for σ_{sl}; a 10% change produces a change in J of 10^2 to 10^3. Viewed in reverse, a measurement of J at some temperature, combined with equation (2.8), provides a basis for determining a surprisingly accurate value of σ_{sl} , a parameter which is very difficult to measure by any other method.

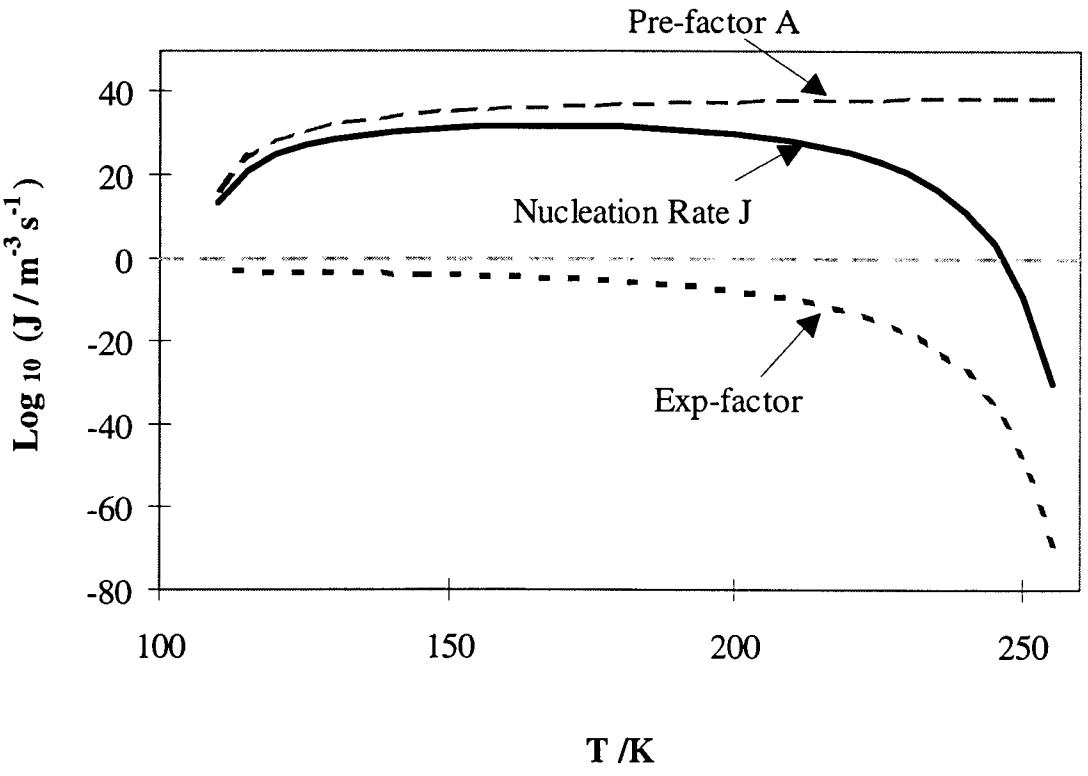

Figure 2-2. Simulation of rate of nucleation for benzene from classical nucleation theory, equation (2.8). Figure shows contribution from exponential and pre-factor separately

Of course, the clusters produced in a molecular jet experience large supercooling before they freeze and the σ_{sl} values are those at the temperature of the initial nucleation. The physical parameters used in equation (2.8) thus have to be extrapolated from known data in the usual liquid region to the supercooled liquid region in order to estimate the interfacial free energy σ_{sl} from equation (2.8). For viscosity,

the following equation,[56] derived from a free volume model, is used to extrapolate the available experimental data for the liquid[57] to the supercooled region.

$$\log \eta = A + B/(T - T_0) \qquad (2.9)$$

In this expression η is viscosity, T is temperature in K, and A, B and T_0 are fitting parameters. Similarly, data for the heat capacity of solid and liquid[58,59] are used to calculate the variation of entropy change with temperature. Linear extrapolation is used to estimate the heat capacity in the supercooled region for the liquid.

The determination of J in an experiment is done as follows. The fraction of solid is easily measured as a function of jet position (time) if we have resolved Raman peaks due to liquid and solid phases, or if electron diffraction patterns with clear indication of solid and liquid phases are seen. The fraction of solid (F_s) is readily obtained from the ratio of the areas of peaks attributed to the solid and liquid phases. F_s as a function of time is used to obtain the rate of solid formation. The rate of solid formation actually has two components; one is the rate of nucleation, the other the rate of solid growth. Since the rate of solid growth is believed to be much faster than the rate of nucleation, the overall rate of solid formation is determined by the rate of nucleation.[9,19] As shown by Bartell, it is easy to derive the following relation connecting the rate of nucleation J to the experimental F_s values[19]

$$Ln\,(1-F_s) = -Jvt \qquad (2.10)$$

By plotting the left-hand side versus time t, we obtain the product of rate of nucleation J and the cluster volume v from the experiment. The latter can be deduced from cooling curves.[13] Hence the rate of nucleation J can be determined from jet experiments. For example, for acetylene, Minarik found a value J = 1.4 $x10^{29}$ m^{-3} s^{-1} for a cluster of diameter 20 nm. The interfacial free energy between liquid and solid σ_{sl} can be derived from equation (2.8). A value of σ_{sl}=10.1 mJ m^{-2} was deduced for acetylene at a supercooled freezing temperature of 155 K.[28]

2.4. Approximate Relation for the Rate of Nucleation

The equation (2.10) has been successfully used to obtain the rate of nucleation for some molecules in electron diffraction, and in some CARS experiments. However, for most molecules investigated either by electron diffraction or by CARS, the time variation of F_s is not directly obtainable. This is because of overlap of spectral peaks or electron diffraction patterns of the liquid and solid phases. The differences between supercooled liquid and solid were found to become smaller, even indistinguishable, with spectroscopy. For benzene, for which the Raman peaks are unresolved for liquid and solid phases in jet, the fraction of solid F_s as an explicit function of time could not be obtained, and hence equation (2.10) was useless.

A modified criterion was devised to determine the rate of nucleation J from the experiment when no distinguishable solid and liquid peak can be obtained. We rewrite equation (2.10) as

$$F_s = 1\text{-}\exp(-Jvt) \qquad (2.11)$$

From this, if a time (t) can be associated with any estimate of the fraction of solid, a rough value for the (Jv) product can be deduced. The rate of nucleation J can thus be obtained if the volume of the cluster (v) is known or can be estimated. We emphasis that even crude estimates of Jv are sufficient to give σ_{sl} to good accuracy.

Completion of the freezing process is more accurately determined in experiments than other time intervals. A plot of F_s versus (Jvt) in equation (2.11) shows that the fraction of solid $F_s = 0.95$ for $Jvt = 3$; hence 95% of the sample is solid, as seen in Figure 2-3. In experiments, this 95% point is about our limit of distinction of the phase transition to solid. The time difference (t) is between initiation and finishing of freezing. We use the criterion $Jvt = 3$ (see Figure 2-3) to get an estimate of the rate of freezing J. This modified criterion is represented by equation (2.12)

$$Jvt = 3 \qquad (2.12)$$

As a test, we applied equation (2.12) to data for acetylene, obtaining $J=2.0 \times 10^{29}$ m^{-3} s^{-1} compared with 1.4×10^{29} m^{-3} s^{-1} from equation (2.10) via fitting the data of fraction of solid F_s as a function of time. Both J values give essentially the same surface tension σ_{sl}, so the use of the simpler criterion for our benzene studies is considered reasonable.

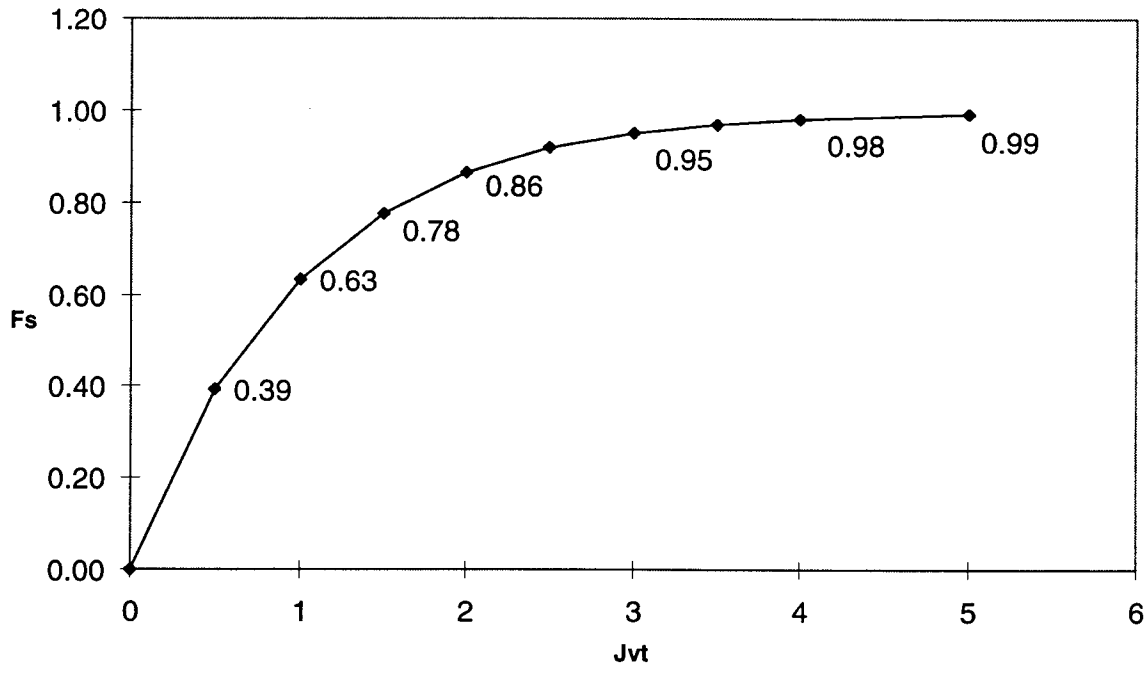

Figure 2-3. Completion of solid fraction Fs versus Jvt.

2.5. Conclusion

The application of classical homogeneous nucleation theory to the phase transition between liquid and solid yields an equation relating the rate of nucleation to the liquid-solid interface. A modified criterion for estimating the rate of nucleation allows us to obtain the rate of nucleation J from information which was not useful before. The interfacial free energy σ_{sl} between liquid and solid benzene will be determined using these relations.

3. EXPERIMENTAL DESIGN AND EXPERIMENTS

3.1. Basic Idea of Experiments

CARS is an acronym for Coherent Anti-Stoke Raman Spectroscopy. The method has high spatial and spectral resolution, and good rejection of background scattered light. The details of CARS theory and applications can be found in reference.[60,61] In this thesis work, we used CARS as a probe to monitor the kinetics of phase changes of molecular clusters in a supersonic jet. Our apparatus consisted of a sample vessel which is used for mixing a benzene sample with a high pressure noble gas, a pulsed nozzle, and a vacuum system. As the valve is pulsed, the molecular clusters form and fly at a high speed as they travel downstream. Lasers are focused on the clusters and spatially moved downstream as the CARS spectra were measured at various positions. The signal was monitored by a photo-multiplier tube (PMT). The wavenumber position of the CARS frequency reflects the temperature and the phase of clusters. To determine the shift of the CARS peaks with temperature, a calibration was done with equilibrium samples where temperature was monitored with a thermal diode. The CARS spectra of these bulk samples, cooled by a cryostat, were recorded to establish this relation.

3.2. CARS System

The experimental results described in this thesis were obtained on the CARS system shown in Figure 3-1. The system consists of lasers, sample handling, and signal

detection sub-systems. The primary laser is a "seeded" Quanta Ray DCR-A Nd:YAG laser which produces a pulsed 1064 nm infrared beam at 10 Hz. The pulses are about 8 ns in duration with a spectral width at best of 0.003 cm^{-1}. The 1064 nm output from the laser is doubled using a 97% deuterated KDP crystal and the resulting 532 nm beam is typically 100 mJ /pulse. One third of the 532 nm beam is used to form two CARS beams, the other two thirds of the 532 beam is used to pump a tunable dye laser. The tunable dye laser is a Lumonics Hyper dye-500 with typical outputs of 5 to 10 mJ per pulse, depending on the dye and the working wavelength. The dye laser pulses have a spectral width of about 0.04 cm^{-1}.

The lasers are focused in a folded BOXCARS geometry. The Anti-Stokes beam generated in this phase-matching arrangement is spatially separated from the pump and probe beams. This spatial separation allows one to direct the weak signal (blue light) through an aperture to discriminate it from the intense green pump and orange probe beams. A holographic filter for the 532 nm light is employed after this spatial filter to further reduce any remaining green light. Colored filters (5-54 Corning glass) may also be used if the amount of background from the dye laser is limiting the instrumental sensitivity. The signal is sent into a McPherson single grating monochromator after the filtering stage. The photons are detected by an RCA 31034 photomultiplier. The output is sent to an SRS SR250 gated integrator, and the integrated signal is digitized with a Scientific Solutions Lab Master A/D conversion board. Data acquisition and dye laser control are achieved through an interface with a 486 PC. More detailed information about the laser and signal detection sub-systems can be found in Minarik's thesis.[28] The

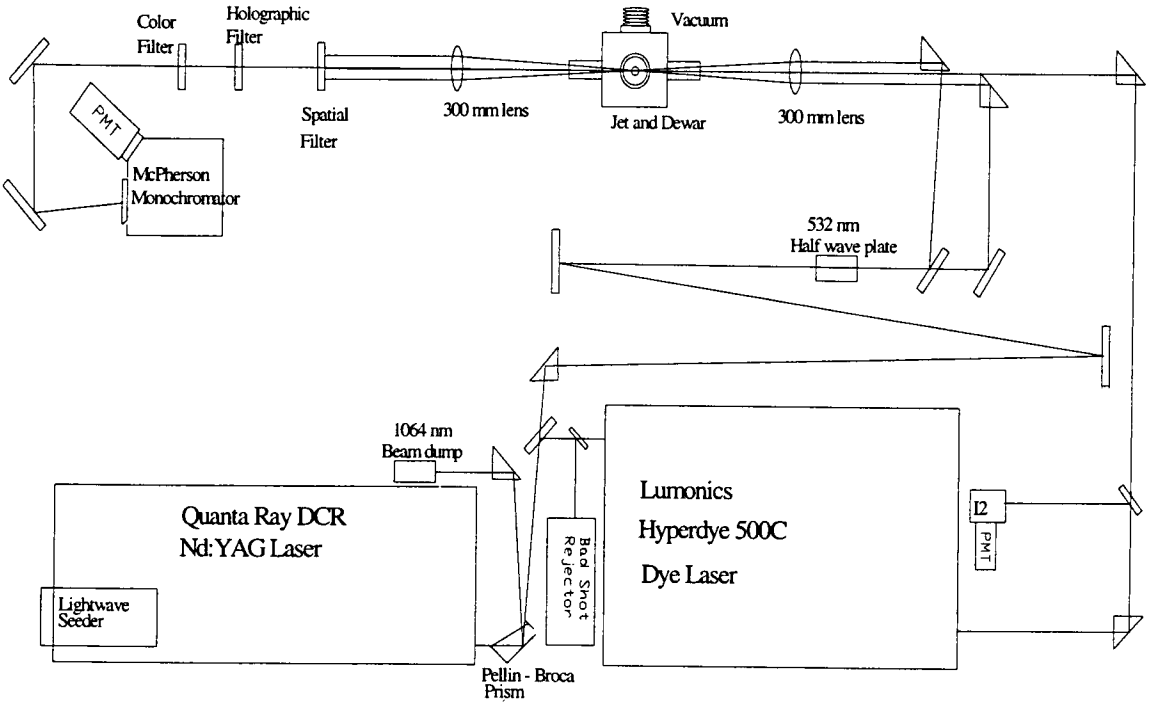

Figure 3-1. CARS experiment set-up for this thesis research

sample sub-system will be discussed in section 3.3. Two critical elements in the laser sub-system and signal detection sub-system are described in some detail below.

3.2.1. Seeder technique for YAG laser

A Nd:YAG laser without any band compression technique typically has a spectral width (FWHM) of about 1 cm^{-1}, a value too broad for the high resolution spectroscopy required for the application in this thesis. The line width was therefore compressed using a "seeder" method.[62] A Lightwave Electronics S-100 infrared diode laser was used to pump a monolithic Nd:YAG crystal to give a single frequency "seed" beam of about 2 mW. This output was injected into the oscillator cavity of the pulsed Nd:YAG laser to produce single mode operation. The spectral width of the laser pulses generated with this "seed" technique is about 0.003 cm^{-1}, which was more than adequate for the experiments described in this thesis.

3.2.2. Bad shot detector

To insure the YAG laser pump frequency stability and to improve the CARS signal to noise ratio, a bad shot detector was added to the system. This detecor is based on an I_2 cell and details can be found in reference.[62] This device eliminates signal contributions from laser shots that are not seeded at a chosen I_2 absorption line (#1109 at 18787.8042 cm^{-1})[63] or are multi-mode. The maximum seeder laser drift is measured to be less than 0.06 cm^{-1}.[64]

3.3. Sample System

3.3.1. Cryostat system for bulk sample

The bulk phase sample of benzene was contained in a sample cell shown in Figure 3-2. This consisted of a copper body screwed into the bottom of the cold finger of an APD Cryogenics HC-4MK1 cryostat. Indium gaskets were placed on the surface of a spacer (about 2 mm) inside the cell and quartz windows were pressed down on the indium gasket to achieve a seal. Liquid samples of benzene were then injected into the spacer through the filling tube. Solids were made by slowly freezing, then approaching the melting point of benzene by warming and then cooling down. This cycle was repeated until an optically clear solid sample was seen. The temperature was then decreased slowly to the lowest temperature that the cryostat could achieve (about 8 K). CARS scans were taken as the sample was warmed from low temperatures to higher ones, allowing continuous scanning until the solid converted to liquid. The temperature was controlled through the use of a Lakeshore 330 Autotuning Temperature controller which was interfaced to a computer.

3.3.2. Molecular jet system for cluster

All of the jet spectra were recorded for expansions produced in a vacuum cell shown schematically in Figure 3-3. In the sample cell the pumping speed is sufficient

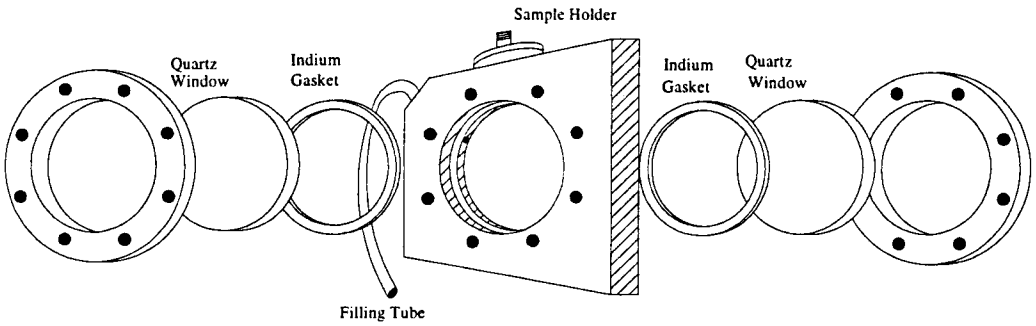

Figure 3-2. Sample cell used in cryostat for bulk benzene

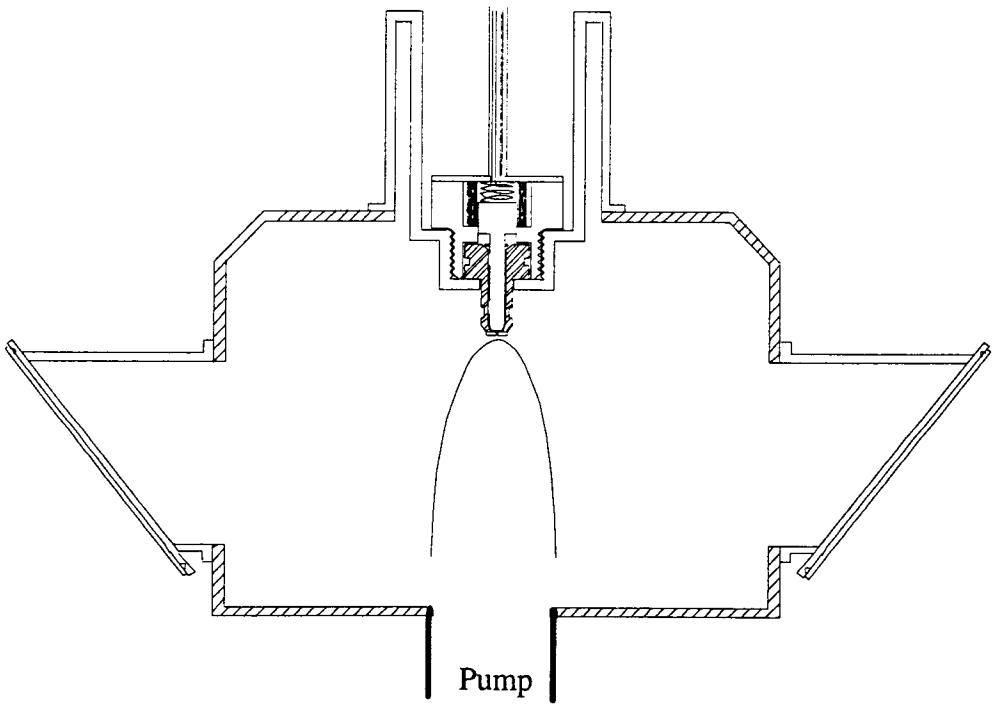

Figure 3-3. Molecular jet

to maintain background pressures (P_b) of less than 1 torr with helium driving gas pressure behind the nozzle at 3.4 or 4.7 atm. Cold free jet expansion conditions are maintained until the gas reaches the Mach disc, where the expansion gas reheats due to background collisions with the background gas. The Mach disc position is a function of the background pressure P_b and the driving gas pressure P_0 behind the nozzle. For gas driving pressures of 3.4 or 4.7 atm, the Mach disc is about 33 or 40 X/D units, where X is the distance from the nozzle and D is the hole diameter. The X/D ranges for the phase transition studies in the free jet are always at positions well before the Mach disc. The jet cell has windows on both side for laser entry and exit for spectroscopy. These windows are held at Brewster's angle so that there is a minimum of reflected light, maximizing the power transmitted through the windows. Mounted inside the cell is a Bosch injector which has been adapted for use as a gas expansion nozzle. The modification includes threading the body for mounting purpose and applying a shim type nozzle to the end. In the case of benzene expansions, two nozzle diameters (0.25 mm and 0.50 mm) were used, in order to allow a wider temperature range of cooling of benzene clusters.

The solenoid of the Bosch injector is driven by a pulse driver which was constructed at OSU. The driver essentially uses an SCR switch to dump the charge of a capacitor through the solenoid windings of the magnetic pulsed valve, at typically 150-350 V. The valve opening is synchronized with the laser pulses by a Hewlett Packard 222A pulse generator, which has variable delay and width capability to provide a clean TTL pulse to the pulse driver. This allowed positioning of laser pulse (10 ns) at about

the midpoint of the about 1 ms jet pulse. Given these widths, the jet can be considered to be a static source on the time scale of the probing lasers.

4. CARS STUDIES OF PHASE CHANGES IN EQUILIBRIUM BENZENE

As the basic unit of aromatic compounds, benzene is an important molecule in chemistry. It is a common solvent and is a typical molecular crystal, crystallizing at 278.4 K. Its solid structure, pictured in Figure 4-1, is orthorhombic with four molecules per unit cell. As mentioned in chapter 1, no other phase transitions in the solid phase have been confirmed by diffraction methods, even though several are suggested by spectroscopic observations. Although our high resolution Raman studies of bulk benzene samples were undertaken primarily to complement our cluster work, the results have some bearing on the questions raised about the structure of the solid. Accordingly some discussion of this aspect is included in this chapter.

4.1. Introduction

Most physical properties of materials are highly related to their phase. A simple example is water and ice, where density and heat capacity differs dramatically in the two states.[65] Knowledge of the various phases of a material as temperature changes is highly desirable to understand the properties of matter. The information of thermodynamics and kinetics of phase transitions is sought by scientist. Various methods are used to study phase transitions; for instance X-ray scattering,[66,67] neutron diffraction,[40] Raman spectroscopy,[68-70] etc Sometimes the problem of detecting phase transitions is difficult and questions arise. As discussed in chapter 1, there is still some controversy about solid state structural change for benzene,[40] such as pre-melting

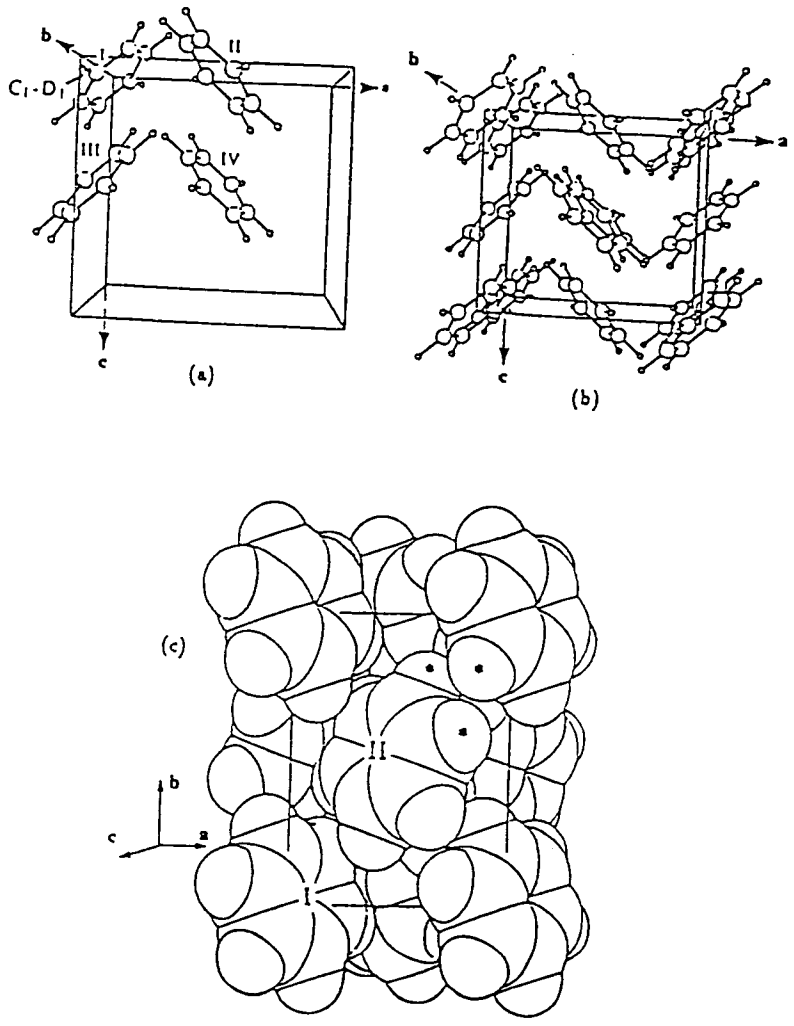

The structure of benzene phase I. (a) "Ball-and-stick" structure of the four molecules in the unit cell; (b) the complete unit-cell; (c) space-filling representation; the surfaces of the atom spheres correspond approximately to the radius of the steep repulsive core of the potential used in the simulations of papers II and III. Note the orientation of the axes in each figure.

Figure 4-1. Structure of solid benzene.[40]

near 278.4 K, a transition to a glass phase around 223 K, and to a low temperature phase around 100 K.

The most interesting issue is perhaps pre-melting. Pre-melting implies that the structure of a solid phase becomes partially modified towards that of the liquid phase as a sample approaches the melting point. The melting of a solid normally occurs such that a solid with an ordered structure changes rapidly into a liquid with a randomly oriented molecular arrangement. The theory of a first-order phase transition predicts that such a transition as melting is abrupt; no pre-transitional effects such as pre-melting are expected.

Some experimental results suggest that pre-melting of benzene might occur. X-ray diffraction of a powder sample of benzene indicates that several diffraction features show large changes of relative intensities as the melting point is approached. This experiment also shows a large expansivity of the lattice parameter $\boldsymbol{c}$ and of the cell volume.[67] These observations are the basis of a claim of a pre-melting effect. Further support comes from Raman spectra that display a marked decrease of frequency of the lattice modes near the melting point,[71] see Figure 4-2. Similar frequency decreases of Raman lattice modes were also observed at non-ambient pressures.[38] Other support for the idea of premelting comes from the measurements of bulk thermal expansivity α_v of molecular crystals near a melting point since these show a power law divergence of α as a function of pressure upon approaching the melting transition.[39]

However, experiments with neutron diffraction for powder samples of benzene[40] failed to detect the effects reported from the x-ray work. The latter effects were argued

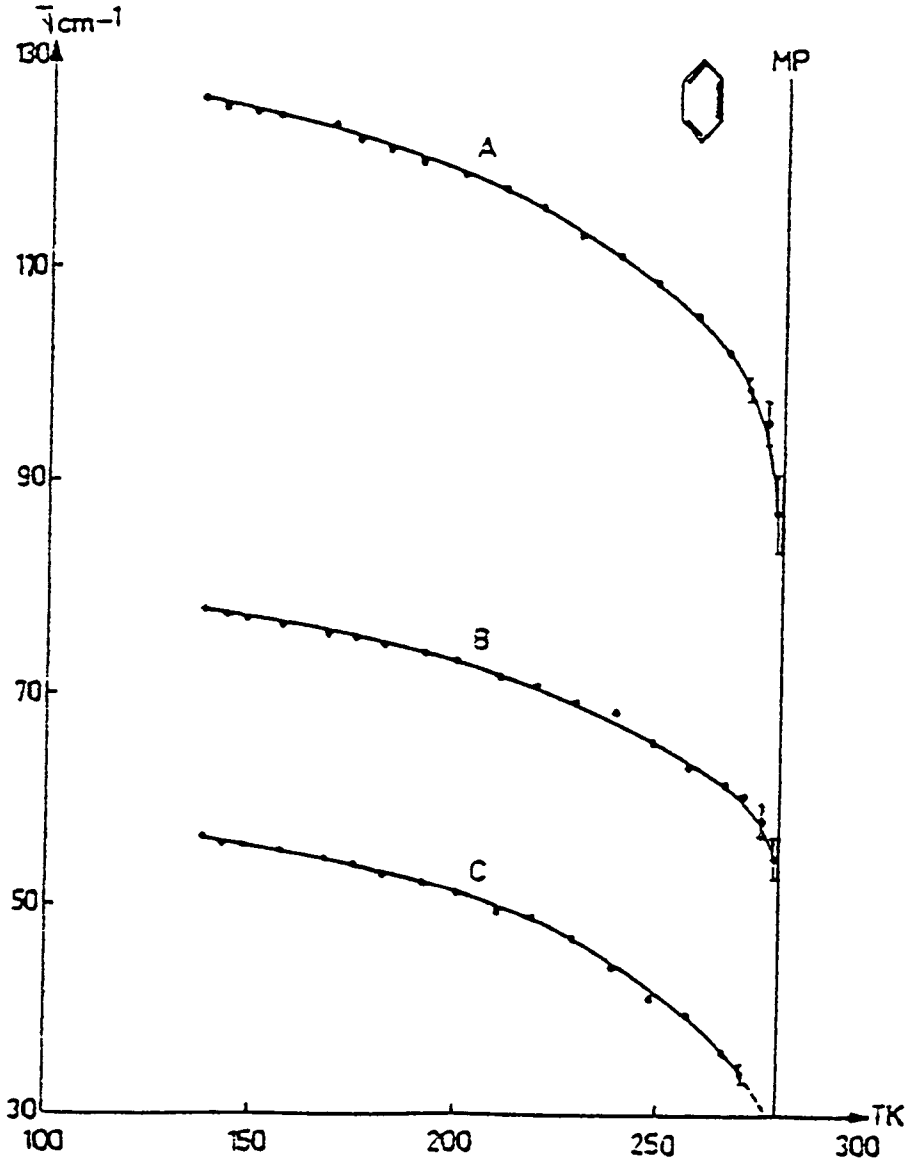

Figure 4-2. Raman spectra of lattice mode near melting point.[71]

to be due to large crystalline samples, and it was suggested that x-ray experiments with a white x- ray source were unsuitable for examination of this question. Concern about impurities and difficulties of working near the melting point prevent the general acceptance of the idea of pre-melting for benzene and for other small molecules.

The concept of pre-melting is of fundamental importance since it affects the common distinction between first and second-order phase transitions. Another interest in pre-melting is that the structure of the pre-melting phase may give insight into the local structure of a liquid, a property which is difficult to determine. Such knowledge may permit construction of a better intermolecular potential energy surface function, which is the foundation of computational physics and chemistry for material properties. Some success has been achieved from theoretical calculations based on intermolecular potential energy surface functions constructed from solid structure data, but a better result can be expected if the potential can be based on intermolecular potential energy surface functions that describe liquid structure data.[12] However little such data are currently available.

Finally, there are some suggestions that solid benzene may exist as a glass or in other crystalline forms. Many organic molecules form glasses and have a glass phase transition.[72] No glass phase has been clearly established yet for benzene, although some researchers have proposed a glass phase transition around 223 K.[73] Other solid phase transitions at 120 K and 100 K have been proposed too. High resolution Raman spectroscopy is a good indicator of phase or structural changes. A series of those spectra of bulk benzene at different temperatures can indicate even subtle structural

changes in the solid material. This measurement is also a necessary part of jet experiments which will be discussed in detail in chapter 5.

4.2. Experiments and Results

4.2.1. Apparatus and sample handling

High resolution CARS spectra were obtained with the system shown in Figure 3-1 and described in detail in chapter 3 and elsewhere.[13] A cell of thickness 2 mm sealed with two quartz windows was filled with benzene (PHOTREX reagent for spectrophotometry, purity 99.9%). The thin cell was then attached to a cryostat (ADP Cryogenics HC-4MK1) where temperature was controlled with a Lakeshore 330 auto-tuning temperature device. The temperature can be maintained with an accuracy better than 0.2 K for a temperature above 100 K. Incident pump and Stokes beams were combined in a Boxcars phase-matching geometry. By fine tuning the overlap of the three laser beams, we generated a CARS signal which was detected with a photomultiplier tube (RCA 31034A). The signal was averaged with a boxcar integrator. A computer received data from the integrator and controlled the scan of the dye laser. To avoid the damage to cell windows and sample burning, reduced powers were used and all laser beams were overlapped in the sample after the focus, such that the diameter of the overlap region was about 1 mm.

The sample was cooled to 275 K, then warmed over the melting point and cooled again for a few cycles to achieve a solid sample of good optical quality. This

step took about two hours. After that, the sample was cooled slowly and, at selected temperatures, CARS spectra were recorded. After each temperature change, the sample was left to stabilize for at least half an hour before the spectrum was recorded.

4.2.2. Spectra and results

The intense ν_2 ring-stretching mode (993.06 cm^{-1}) of benzene[74] was the focus of all spectral measurements. The spectra recorded during the cool-down process can be seen in Figure 4-3. Over a period of 12 hours the temperature was lowered to 8 K. Then, the sample was warmed, and spectra were recorded at selected temperatures. The spectra recorded during the sample warm-up process can be seen in Figure 4-4. Again after each temperature change, the sample had at least half an hour to equilibrate. Special attention was paid to measurements near the 278.4 K melting point of benzene. The sample of benzene was visually solid inside the sample cell of cryostat before and after the spectra were recorded at all times at 278.2 K and lower. When the temperature control was released near 278.2 K, benzene melted and a mixed sample of solid and liquid appeared. Efforts to record the CARS spectra of this sample were not successful, presumably due to fluctuations as solid moved in and out of the overlapped beams.

Spectra of the liquid and of vapor in a separate cell were also recorded for comparison and for calibration purposes. The latter is necessary because of some variability of the dye laser reading when it is adjusted for maximum power of different laser dyes. The Nd:YAG frequency was taken to be 18787.804 cm^{-1} since the seeder was tuned to match the iodine vapor line #1109 at this value. The dye laser correction

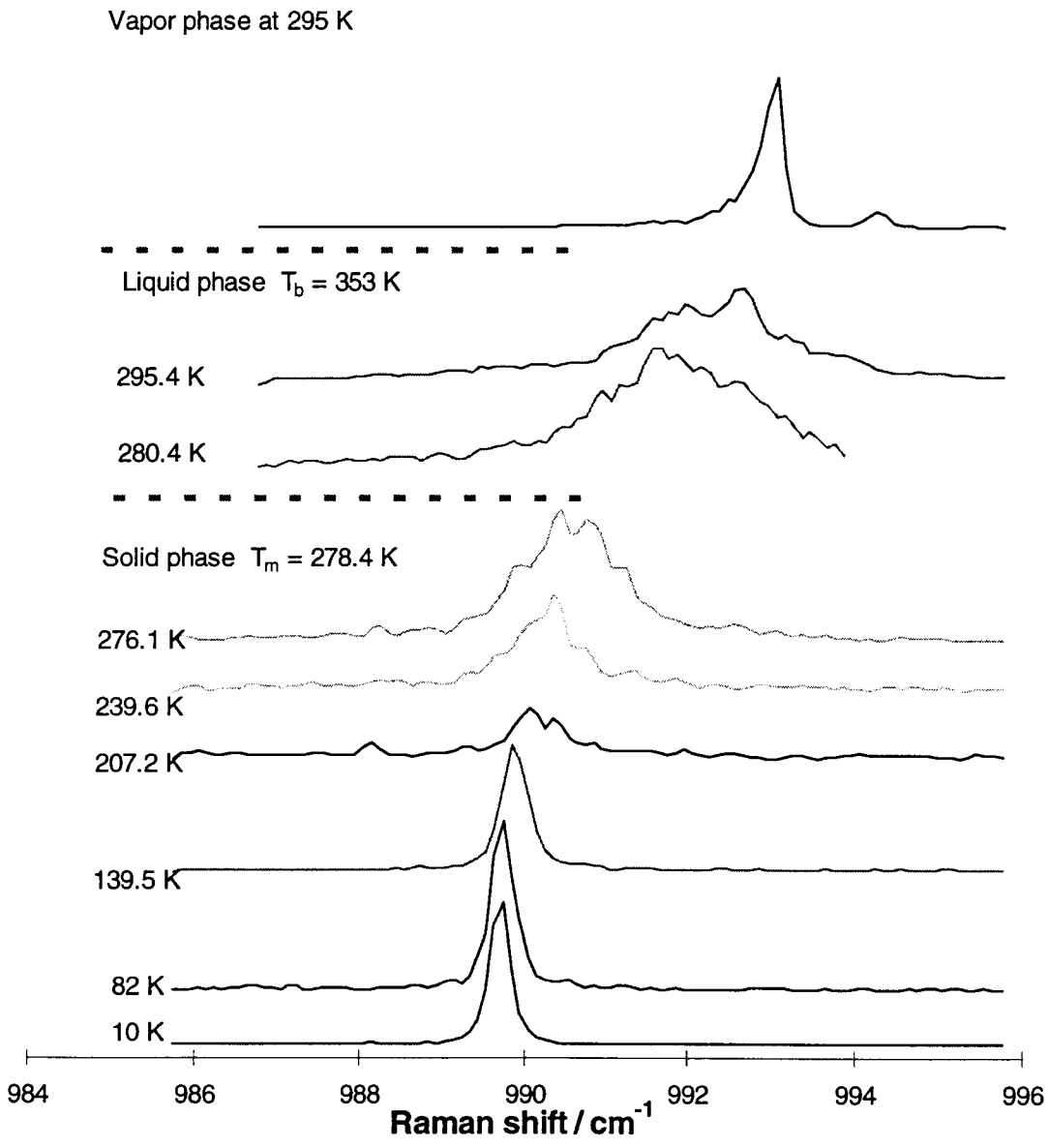

Figure 4-3. CARS spectra of benzene in a cryostat for a cool-down sequence. The vapor spectrum was recorded in a separate cell.

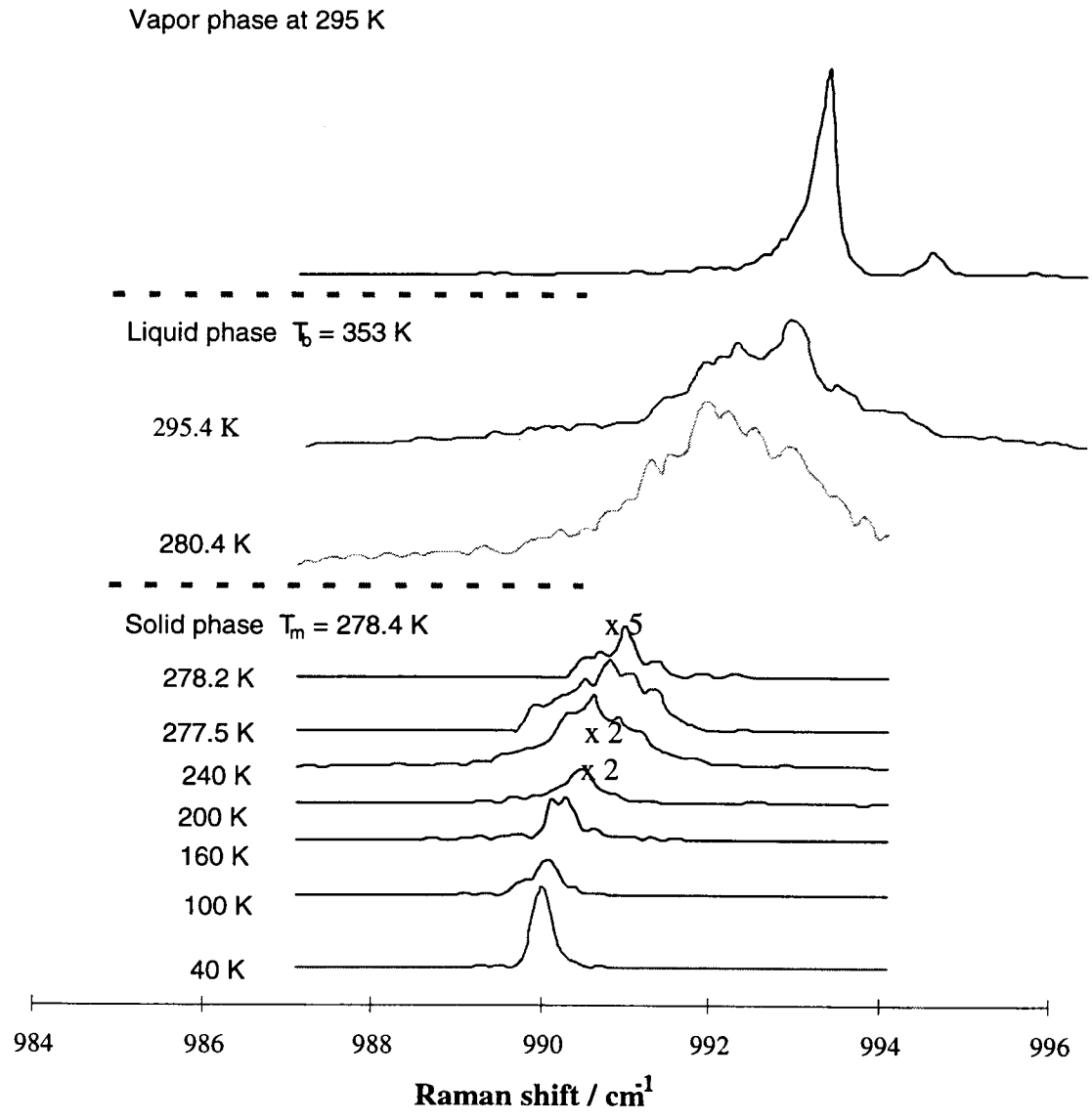

Figure 4-4. CARS spectra of benzene in a cryostat for a warm-up sequence. The vapor and liquid spectra are the same as in figure 4-3.

was then deduced from the measured Raman shifts of the maximum of the unresolved Q branches of CO_2 and benzene vapor; Table 4-1 summarizes these measurement. Since it was most appropriate for the spectral region of our measurements, the benzene vapor correction of 2.93 cm^{-1} was used in obtaining the Raman shifts listed in Table 4-2 for the condensed phases of benzene.

4.2.3. Analysis

Each spectrum in Figure 4-3 and 4-4 was fitted using the program Peak-Fit to obtain the peak center, the width of the peak (FWHM), and the intensity (represented by the peak areas of the bands). These quantities are plotted versus temperature in Figure 4-5 to 4-7 for the cool-down/warm-up sequence. The error bars for the widths (Figure 4-6) corresponds to two times the fitting standard error. Since the Raman shifts in Figure 4-5 were determined by the calibration of gas phase, and solid or liquid phase peak positions, those error bars were calculated as twice the square root of the summation of squares of the standard error for gas and condensed phase peaks. All the data are summarized in Table 4-2.

The Raman shift versus temperature relation (Figure 4-8) was established with the warm-up sequence data. Tthe solid and liquid lines show fits of the peak center position data to the following functions.

Liquid $\quad T = -43182.16 + 43.82144\, \nu_2 \quad (4.1)$

Solid $T = -172028874.97 + 347262.96919\ \nu_2 - 175.24869628\ \nu_2^2$ (4.2)

In the case of the solid, only data above 100 K was used for the quadratic regression. (An excess of significant figures is enable given to calculation of temperature to 0.1 K). These functions will used in chapter 5 to convert liquid/solid cluster peak center positions to temperatures.

Table 4-1. Summary of spectrum calibration data of CO_2 and benzene vapor.

Molecule	Raman cm^{-1}	STD Error	FWHM cm^{-1}	STD error	Peak area
CO_2	1282.44	0.003	0.178	0.007	2.1
at 293 K	1282.45	0.003	0.221	0.006	2.4
200 torr	1282.53	0.003	0.269	0.005	2.2
Ave.=	1282.47	0.003	0.222	0.006	2.2
Correction[a]	3.04				
Benzene					
at 293 K	990.05	0.005	0.307	0.008	2.6
80 torr	990.01	0.004	0.281	0.005	1.9
vapor	990.01	0.005	0.298	0.006	1.4
Average=	990.02	0.005	0.295	0.006	2.0
Correction[b]	2.93				

a) Measured assuming the unresolved Q-branch maximum is at 1285.51 cm^{-1}
b) Measured assuming the unresolved Q-branch maximum is at 992.95 cm^{-1}
This correction was used in deducing the Raman shifts of liquid and solid benzene in table 4-2 .

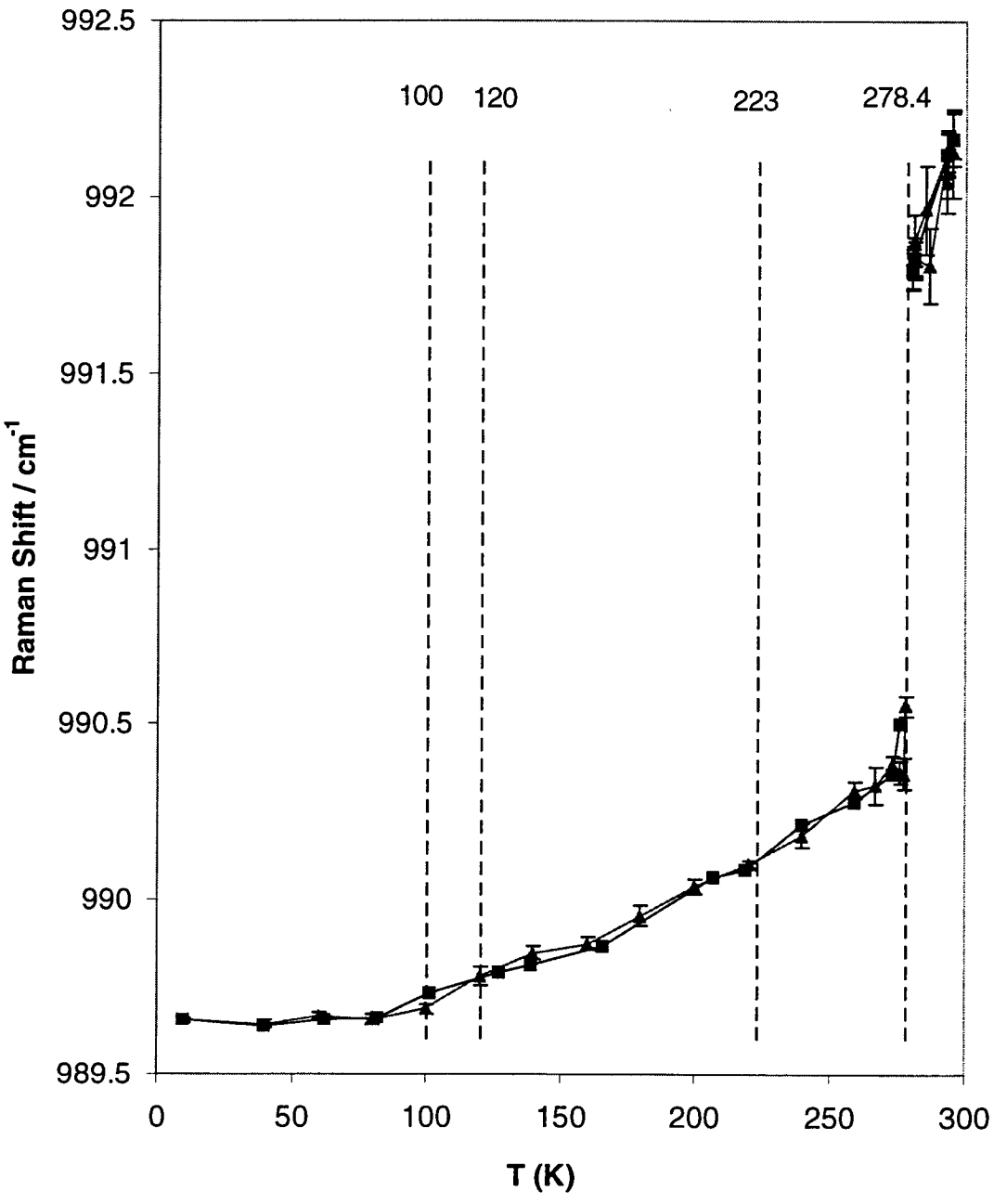

Figure 4-5. Raman shifts of warm-up and cool-down sequence. Triangles are warm-up data, squares are cool-down data.

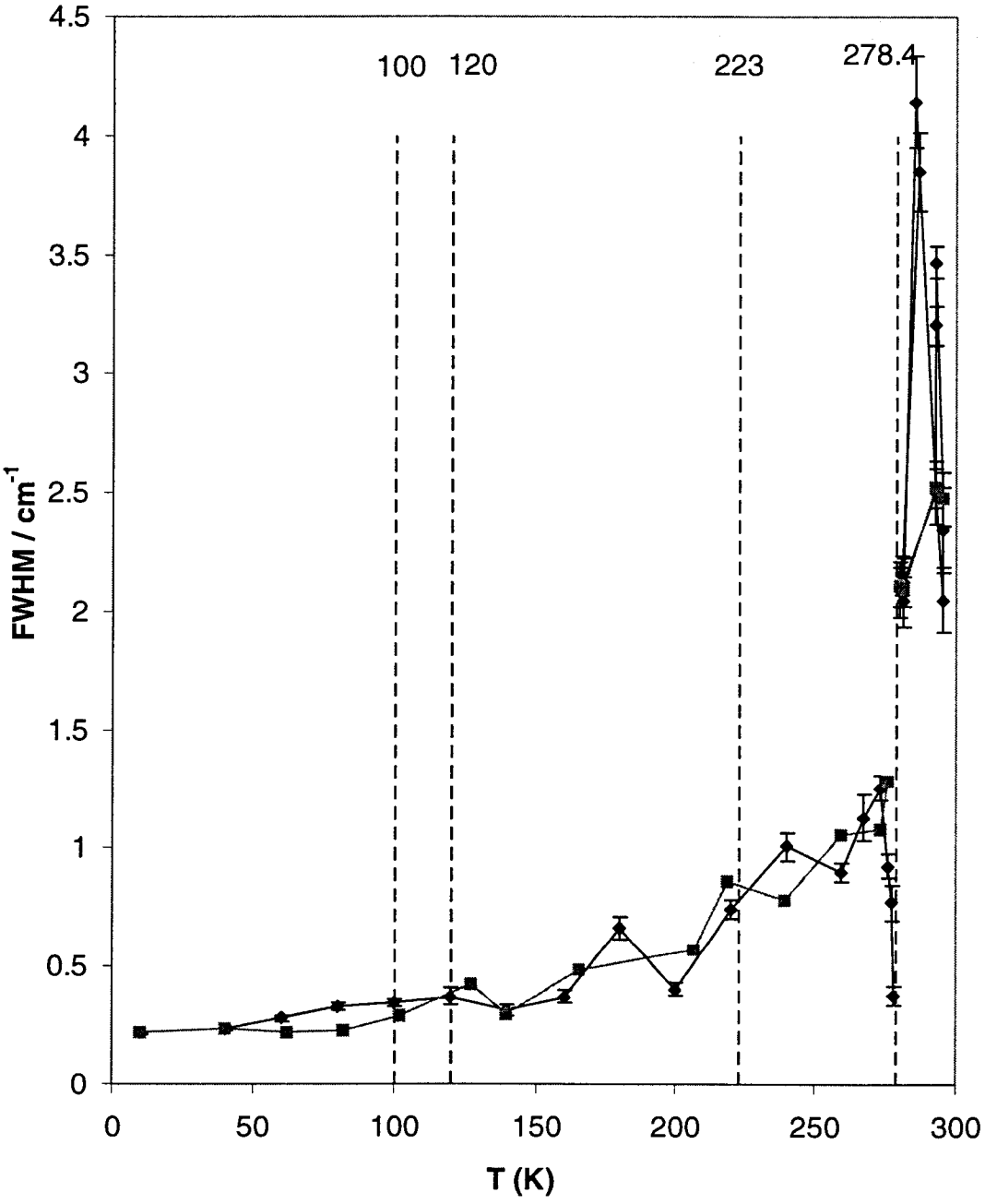

Figure 4-6. Linewidth of CARS peaks of warm-up and cool-down process. Triangles are warm-up data, squares are cool-down data.

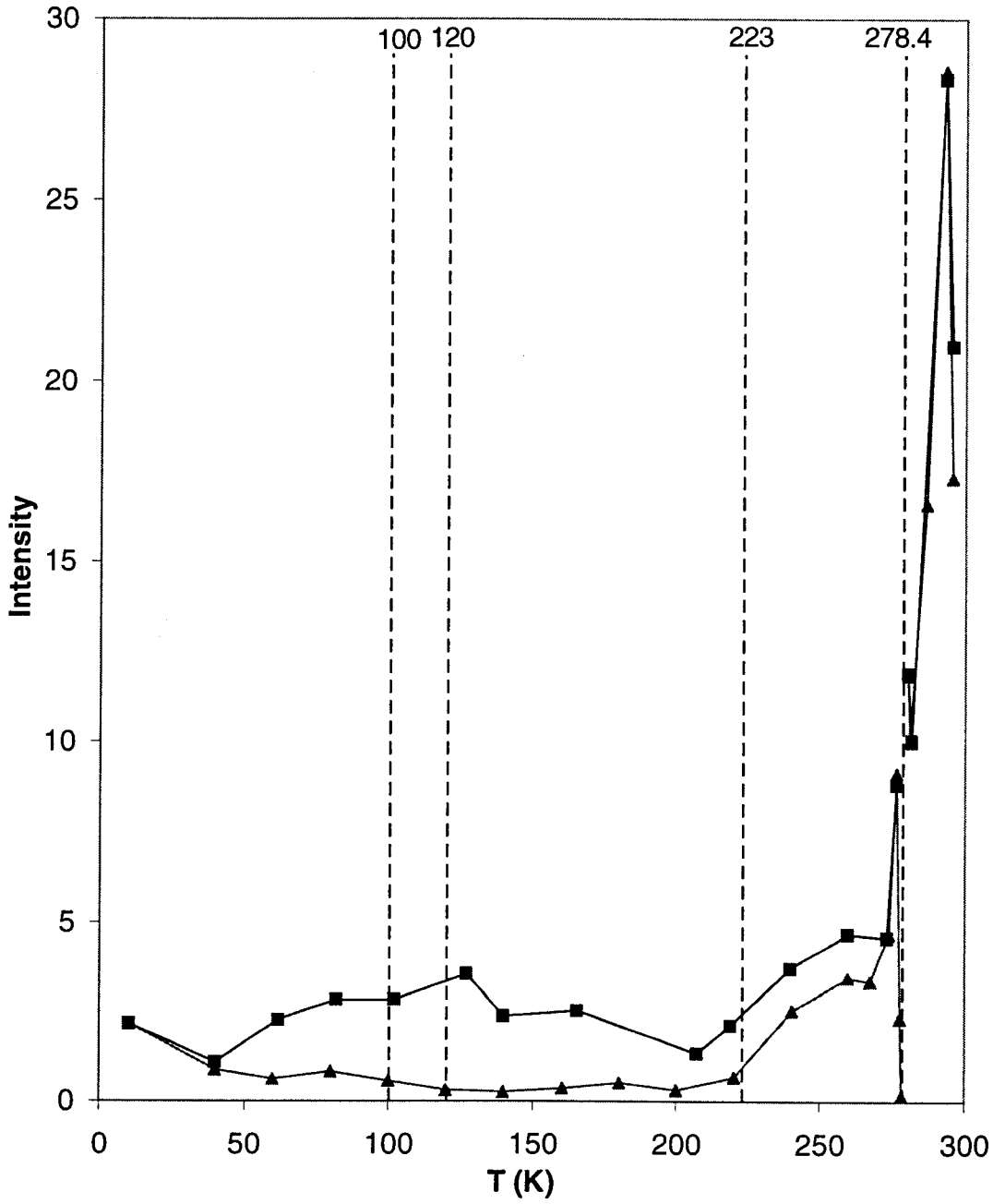

Figure 4-7. Intensity of CARS peaks of warm-up and cool-down sequence. Triangles are warm-up data, squares are cool-down data.

4.3. Discussion

4.3.1. Solid-liquid phase change

In the gaseous phase, the Raman shift of the free molecule is 993.06 cm^{-1} for the ν_2 symmetric ring stretch mode,[74] whereas, in the liquid and solid phases, because the molecule is in a local field of other molecules, the Raman shift is altered. The attractive or repulsive forces in condensed materials produce a red or a blue shift of Raman lines from the gaseous phase.[13] If the Raman shifts are smaller in the condensed phases than those in the gaseous phase, attractive forces are responsible, such as in benzene. The attractive force between molecules is a continuous function of temperature in the solid phase, which should give a continuous change of Raman shift with temperature.

As the local fields of liquid and solid are different, we see a step discontinuity of the Raman shift as the liquid freezes to the solid, as in Figure 4-5. Similarly, there are obvious discontinuities in the linewidth and peak intensities at 278.4 K (Figure 4-6 and 4-7). All observations are consistent with a first order phase change and the fact that the changes occur right at the known melting point indicates that the sample is quite pure.

Table 4-2. Summary of Raman shift, width, and intensity of bulk benzene sample

T K	Raman cm^{-1}	STD error	FWHM cm^{-1}	STD error	Peak area
Liquid					
295.4	992.180	0.033	2.05	0.068	17.3
293.0	992.134	0.029	2.50	0.065	28.3
281.2	991.830	0.025	2.12	0.052	10.0
280.4	991.801	0.027	2.09	0.060	11.8
Solid-cool down					
276.1	990.504	0.018	1.29	0.031	8.8
273.1	990.360	0.016	1.08	0.028	4.6
259.2	990.282	0.018	1.06	0.030	4.7
239.6	990.214	0.015	0.78	0.024	3.7
218.7	990.090	0.019	0.87	0.031	2.1
207.2	990.068	0.013	0.57	0.021	1.4
165.5	989.870	0.007	0.48	0.010	2.5
139.5	989.816	0.002	0.30	0.003	2.4
127.0	989.793	0.004	0.42	0.006	3.6
101.5	989.738	0.003	0.29	0.003	2.9
82.0	989.669	0.003	0.23	0.004	2.8
62.0	989.659	0.002	0.22	0.003	2.3
40.0	989.640	0.002	0.24	0.002	1.1
10.0	989.660	0.001	0.22	0.002	2.2
Solid-warm up					
278.2	990.557	0.014	0.38	0.019	0.1
277.5	990.361	0.022	0.77	0.038	2.3
276.2	990.367	0.015	0.93	0.027	9.1
273.7	990.384	0.013	1.26	0.025	4.7
267.1	990.328	0.026	1.13	0.048	3.4
259.3	990.314	0.012	0.90	0.021	3.5
240.0	990.186	0.017	1.01	0.030	2.5
220.0	990.104	0.001	0.75	0.019	0.7
200.0	990.041	0.009	0.40	0.014	0.3
180.0	989.955	0.014	0.67	0.024	0.5
160.0	989.876	0.008	0.37	0.013	0.3
140.0	989.849	0.009	0.32	0.013	0.3
120.0	989.783	0.012	0.37	0.018	0.3
100.0	989.693	0.005	0.34	0.008	0.5
80.0	989.661	0.006	0.33	0.009	0.8
60.0	989.674	0.003	0.28	0.005	0.6
40.0	989.648	0.004	0.24	0.004	0.9
10.0	989.660	0.001	0.22	0.002	2.2

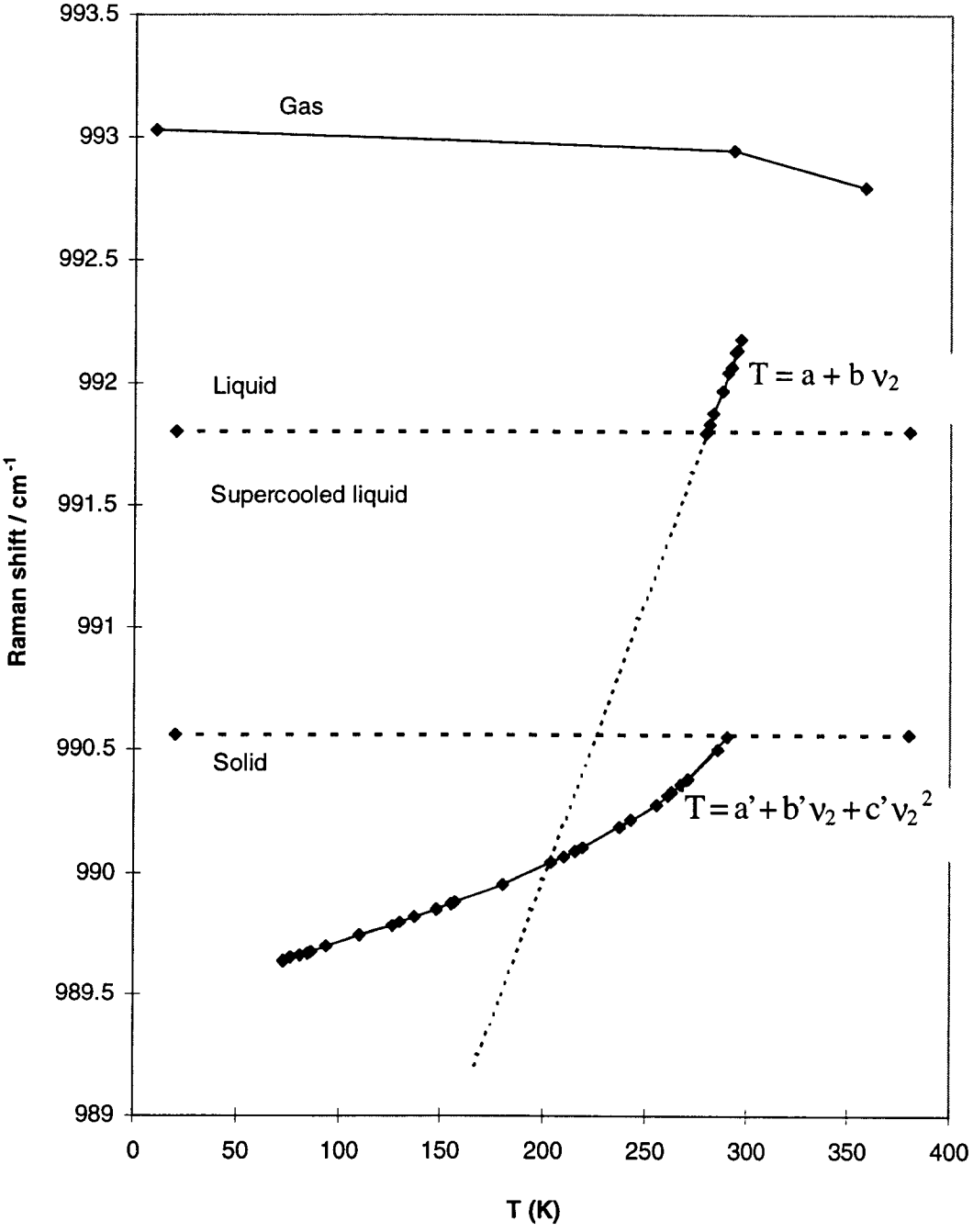

Figure 4-8. Raman shift versus temperature relation for bulk phases of benzene.

4.3.2. Glass phase change

Existence of a glass phase for benzene has been proposed based on IR observations, which show an absorption peak splits into a doublet as the temperature cools over 223 K.[73] In our experiments, we do not see near this temperature any obvious discontinuity in the solid Raman shift or in the linewidth plots for either the cool-down or warm-up sequence, Figure 4-5 or 4-6. Also, neither figure shows any indication of hysteresis, which is typical for a glass phase transition for cool-down/ warm-up curves.[75] The intensity curves (Figure 4-7) do show a general increase with warming above 200 K but the errors in this quantity are large and, in any event, other factors could produce this rise. Overall, the existence of a glass phase is not supported by our CARS measurements.

4.3.3. Other proposed solid phase changes

As mentioned earlier, a phase change at ~ 100 K was proposed from neutron diffraction,[66] and was disputed by another experiment.[40] Measurements of the spin-lattice relaxation times and the width of the nuclear magnetic resonance absorption line gave evidence of molecular re-orientations (not free rotation) about the sixfold axis at ~120 K.[41] In our experiments, we do see that the plot of Raman shift versus T gives different slopes below and above 100 to 120 K so some such reorientational process may indeed be occurring. There is no abrupt linewidth or intensity change in this region however. These plots do seem to show an increase at temperatures above 200 K. This trend offers some support for the NMR measurements[41] which showed, by a departure

from a linear relationship between $\log(\tau_c)$ and $1/T$, evidence of increased reorientational motion above 240 K. None of these changes appear to be abrupt, as in the case of melting at 278.4 K, so any structural changes are likely to be minor.

4.3.4. Existence of a premelting process

As noted earlier, there has been some dispute about whether a pre-melting process, or phase, might exist 1-2 K below the true melting temperature. Thus it may be significant that there is a small but clear jump in the solid frequency just below the melting point in the solid phase in Figure 4-5 for both cool-down and warm-up sequences. The width of the solid peak near the melting point also shows a distinct narrowing during for the warm-up process of Figure 4-6. A sudden change of intensity can also serve as an indicator of a phase transition,[67,76] and, indeed, the intensity of the CARS peak shows marked changes about 1 K below the melting point, as shown in Figure 4-7.

Two possible explanations for these observations come to mind. First, because the temperature is so close to the melting point, benzene might be partially liquid and partially solid, or in a condition of solid-liquid co-existence.[34,77,78] Second, there could be an actual structural change in the solid phase corresponding to pre-melting. Below, we consider these in turn.

The question of co-existence of liquid and solid phase is interesting.[79,80] It is possible that benzene molecules absorb energy from the laser beams, leading to partial melting of the solid sample at the laser focus volume. This process could produce a

mixture of a small amount of liquid in the solid sample which, if the peaks are broad and overlap, could produce the drop in Raman shift of the solid that we see in our experiments on bulk samples in the cryostat. This melting would not be seen visually since the sample is not easily viewed during the intense laser pulse. Of course, benzene has no strong absorption bands near the wavelengths of our CARS system, which are at 532 and 560 to 570 nm. However, benzene has a strong absorption near 220 nm, so that absorption of two photons of 532 nm light is possible at the tail of this band. Also, stimulated Raman pumping to the $\nu_2 = 1$ level is produced at the same time as the CARS signal is generated so there will be some heating by this process. Both the two photon absorption and stimulated Raman processes are much weaker than one photon absorption, but their occurrence to an extent which could partially melt benzene sample can not be excluded.

Nonetheless, we do not think it is likely that such multiphoton processes occurred in these experiments because we used a loosely focused beam to avoid sample burning in the cryostat, a defocusing condition which works strongly against such multiphoton processes. Also, on examining Figure 4-6, we see that the width of the solid peak decreases close to the melting point, whereas a contribution by a liquid fraction would cause an increase since the liquid peak is twice as wide as the solid peak. Finally, we have not seen evidence of sample melting at the laser focus in similar experiments on acetylene and other molecules. Overall, our data is not inconsistent with the idea that pre-melting starts at about 1 K below the melting point, as suggested by x-ray scattering.[67]

What would be the nature of a pre-melting step? This is difficult to answer but it presumably involves an increased amplitude of vibration of some lattice modes in the crystal, which modifies the environment of internal mode ν_2 and causes it to change. Since the ***c*** axis expands the most just below the melting point, the mode must have an amplitude component along ***c*** axis. Examination of Figure 4-1 shows that the linkage from one benzene to another along the **c** axis involves overlap of the pi electrons of the nearly parallel benzene rings. This interaction would be weakened if a gear-like rotation occurred about the six fold axis of each benzene. This would result in a preferential increase in the **c** axis dimension, as observed in the x-ray study.[35]

4.4. Conclusions

Our high-resolution CARS spectral measurements on benzene in a cryostat give Raman frequency versus temperature relations which will be used in the cluster studies in chapter 5. Some indication are seen for proposed phase changes in solid benzene from 278.4 K down to 8 K. There is evidence to indicate minor structure changes at 240 K and at 100-120 K but none for a glass phase change of benzene around 220 K. Support for the concept of premelting in the case of benzene comes from some spectral changes seen just below the melting point. This work demonstrates that CARS is a useful tool which can contribute to the understanding of phase transitions of solid.

5. CARS STUDIES OF BENZENE CLUSTERS FORMED IN JET EXPANSIONS

Liquid benzene clusters of about 10 nm in diameter were formed in a supersonic jet and monitored by CARS spectroscopy. These droplets supercool to a temperature estimated to be around 230 K and partially froze into solid particles, causing warming due to the heat of fusion. This warming effect was discerned from subtle peak shifts in the CARS spectra which served as an indicator that the freezing phase transition had occurred over a period of about 0.4 μs. The interfacial free energy between liquid and solid benzene, σ_{sl}, is calculated by using homogeneous nucleation theory combined with the jet experimental data and is compared with the other limited data available in the literature.

5.1. Introduction

Nucleation of condensation, freezing, and solid-solid phase transitions lies at the heart of catalysis, metallurgy, materials engineering, earth science, etc. The kinetics of homogeneous nucleation constitutes the key to understanding such processes. The main parameter which links experiment and theory is the interfacial free energy (σ, surface tension). Because of the difficulty of achieving homogeneous nucleation of freezing and experimentally measuring the liquid-solid surface tension, we know much less about freezing than its importance in our daily life and science dictates. The reason is not that the theory is primitive, but that truly homogeneous nucleation experiments are extremely difficult to perform. Trace impurities always exert a large influence.[5,6] There

are few truly homogeneous experimental data that one can use to compare with homogeneous nucleation theory. Therefore appropriate homogeneous nucleation experiments are valuable for the understanding of nucleation of freezing and for the development of nucleation theory in condensed phases.

Molecular clusters, with diameters from 5 nm to 50 nm, produced in a supersonic jet, are considered a satisfactory homogeneous sample ensemble. Their physical and chemical properties resemble closely those of a bulk sample[15] and non-intrusive techniques are available to measure the temperature of the ensemble and to monitor changes in phases. In particular, these methods are electron diffraction by the group of Bartell[16,18,19] and CARS in our group.[13,14] Most of the molecular clusters formed by Bartell in his jet were supercooled liquids, including benzene.[18] In a few cases, solid clusters formed from supercooled liquid.[13,14,16,19] In two studies by coherent laser spectroscopy (SRS and CARS), solid clusters of nitrogen and acetylene have been seen in a supersonic jet and their kinetics followed. These are advantageous cases since spectral features were resolvable into two peaks, one representing liquid and the other solid, so it was possible to monitor the process of freezing in the jet.

However, not all systems give two resolved peaks which can serve to indicate a liquid-solid phase transition. Often the spectral separation between peaks due to liquid and solid phases diminishes as the clusters supercool, leading to overlap, as we found for benzene. A different indicator, which is suitable for the study of nucleation of freezing in most molecules, is needed to indicate the onset of freezing in a jet. Thermodynamics tells us that if any supercooled liquid freezes into a solid at a supercooled temperature (T_L), the liquid-solid system will warm rapidly, usually to the

melting point (T_m) unless the system has extreme supercooling. The difference between T_m and T_L can be large in a jet as the aggregate experiences rapid cooling in the expansion process.[13,14,19,32] Detection of a temperature rise can thus serve to indicate the onset of the freezing process. A small variation of Raman shift due to the temperature rise of the supercooled liquid and solid mixture can be monitored with CARS.

In this thesis, benzene is used to demonstrate experimentally that this indirect detection of freezing is feasible and the advantages and limitations of this approach are discussed. The theoretical expression for the rate of nucleation, discussed in chapter 2, is used in this work to deduce the surface tension σ_{sl} between liquid and solid benzene.

5.2. Experiments

5.2.1. Molecular free jet cooling mechanism

Underexpanded beams emanating from sonic (shim) nozzles are generally termed free jets. The isentropic expansion (as occurs in free jets) leads to decreasing gas density and translational temperature with increasing distance from the nozzle. Density and gas temperature decrease until the expansion reaches the background pressure, where cooling collisions have essentially ceased. Because of the rapid cooling in free jets, there may be regions of the expansion zone characterized by local pressure higher than the correspond vapor pressure of a condensed phase. This supersaturation leads to clustering if the time remaining before the expansion runs out of collisions is

sufficiently long. Note that, because of cohesive energy being released, the onset of clustering heats up the beam.

Three factors determine the extent of clustering in free jets: stagnation pressure, aperture cross section, and initial gas temperature. In general, cluster concentration as well as average cluster size increase with stagnation pressure and cross section of the nozzle, whereas they decrease with increasing reservoir temperature. Expansions from smaller nozzles have fewer molecules to be clustered and run out of collisions sooner; hence smaller clusters are formed. For the same reason, expansions from smaller apertures typically have much higher cooling rates than are found for larger orifices. Note that, for small nozzle cross sections, beam divergence and translational temperature increase.

After the onset of clustering, the cooling of clusters produced in supersonic beams can proceed by two microscopically distinct mechanisms. The first is collisional cooling, that is, the relaxation of internal degrees of freedom by two-body collisions to the monomers and/or the carrier gas. This mechanism is effective up to the Mach disc location. The second mechanism is evaporative cooling, which proceeds throughout the time of transit up to the detection point, even after collisional cooling has ceased. RRK theory predicts that evaporative cooling is important at a cluster temperature of $0.3\ \varepsilon / k < T < 0.6\ \varepsilon / k$, where ε is the binary binding energy between two molecules in the cluster and k is the Boltzmann constant. Further details about free jet theory and applications to cluster studies can be found in references.[81]

5.2.2. Free jet experiments with benzene

The CARS system and free jet apparatus used to study supercooling and kinetics of freezing has been described in detail in chapter 3 and elsewhere.[13] The pulsed nozzle is a shim type, with a diameter D either 0.5 mm or 0.25 mm. The thickness of the shim was 0.5 mm for both nozzles. Instead of the loose beam overlap used in the cryostat experiments (chapter 4), in the jet experiments all laser beams were tightly focused with a lens (focal length 300 mm); the diameter of the focus was about 0.1 mm. The typical laser energy is about 15 mJ for YAG beams, and about 5 mj for the dye laser beam. Our CARS system has a spectral resolution about 0.05 cm^{-1}.[64]

The same benzene sample employed in the cryostat experiments (PHOTREX reagent for spectrophotometry, purity 99.9%) was used in the jet measurements. The experimental conditions were varied to change the extent of clustering produced at large X/D distances, at increased helium driving pressures, and with smaller diameter nozzles. Initially, pure benzene vapor was used. Serial spectra versus X/D, accomplished by lifting the whole jet instead of moving the laser beams, were recorded until the signal was too weak to be seen. Next, helium (purity 99.9%) at a driving pressure of 1.7 - 4.7 atm, was bubbled through liquid benzene at 295 K, forming a mixture which was expanded into the evacuated chamber through the pulsed nozzle.

5.2.3. Determination of cluster temperature by Raman shift

The temperature of the clusters is one of the key parameters we need to determine for the study of supercooling and kinetics of freezing. We have mentioned in

chapter 4 that the Raman shift versus temperature relation established for bulk samples can be used to determine the temperature of clusters in our free jet, since these clusters contain more than 1000 units, i.e. are bulk-like. In the jet experiments, the monomer and cluster peaks can be recorded in the same spectral scan. The monomer position is a very good reference for calibration purpose because the benzene ν_2 band is an intense and narrow feature and its position in the jet is nearly constant during an experiment, see Table 5-1 to 5-5. In comparing with jet experiments, we use the bulk results of Figure 4-8, in which the Raman shift is plotted versus temperature. In the bulk sample experiments, the reference point is the room temperature monomer peak maximum position, while in the jet experiments it is the cold monomer peak position. The ν_2 peak center position has been determined to be 992.80 cm^{-1} for benzene vapor at 85 C and the Q_0 band head position has been deduced to be 993.06 cm^{-1}.[82] Our peak center position of benzene vapor for the calibration of cryostat data was determined at 22 C, which we estimate should be around 992.95 cm^{-1},Table 4-1. We assign the peak center position in the jet as 993.03 cm^{-1}, a reasonable shift since the sample is colder than room temperature. With these reference points, the Raman shift of the clusters can be used to deduce temperature from the equations (4.1) and (4.2) for liquid and solid respectively.

5.3. Results and Analysis

5.3.1. Pure benzene vapor in a jet

Two experiments were done involving expansions of neat benzene. One was at 295 K, room temperature, where benzene has a vapor pressure of 82 torr. The second was at 335 K where the pure benzene vapor pressure is 416 torr. No cluster peaks were seen in either pure vapor jet experiments. Sample spectra of pure benzene vapor at 295 K and in a jet are shown in Figure 5-1 for a large nozzle jet (D = 0.5 mm), and in Figure 5-2 for a small nozzle jet (D = 0.25 mm) with benzene vapor at 335 K. We conclude that pure benzene vapor in a jet is not able to cool sufficiently to condense or freeze to produce liquid or solid clusters. However, we do see the effects of cooling in the jet. The width of the vapor peak narrows and the peak center shifts to slightly higher Raman values, implying cooling as X/D increases, see Table 5-1. The peak at 994.2 cm^{-1} is a hot band $(\nu_2+\nu_{20})-\nu_{20}$;[82] its intensity relative to that of ν_2 decreases as cooling occurs in the jet, Figure 5-1 and 5-2. Interestingly, this hot band is still present at X/D up to 5 in the large nozzle jet, Figure 5-1, but it is gone even at X/D = 0.4 in the smaller nozzle jet, Figure 5-2. The widths of the peaks are also narrower in Figure 5-2 compared to Figure 5-1. It can be concluded that, at the same X/D positions, the jet with a smaller diameter nozzle produces a much colder molecular beam compared to the jet with a large nozzle.

Even though the frequency shift is very small for benzene vapor in the jet, we can see that it initially increases, then decreases as X/D increases. This means the molecules cool down first, then warm back up. This cooling and warming effect can

also be spotted in the width of the peak, which shows a decrease first, then an increase, see Table 5-1. This effect can be attributed to the small zone of free flow for a low pressure expansion. This extends to the Mach disc location; after the molecules reach this location they collide with the background gas, which warms them up. The Mach disc position of a jet is determined by the driving pressure (P_0) and the background pressure (P_b) in the vacuum chamber according to the relation[81] $X/D = 2/3\sqrt{P_0/P_b}$. The background pressure is about 1 torr in our system, putting the Mach Disc limit at 6 X/D units when the benzene sample is at 295 K. Warming at about this position is consistent with our experimental observations.

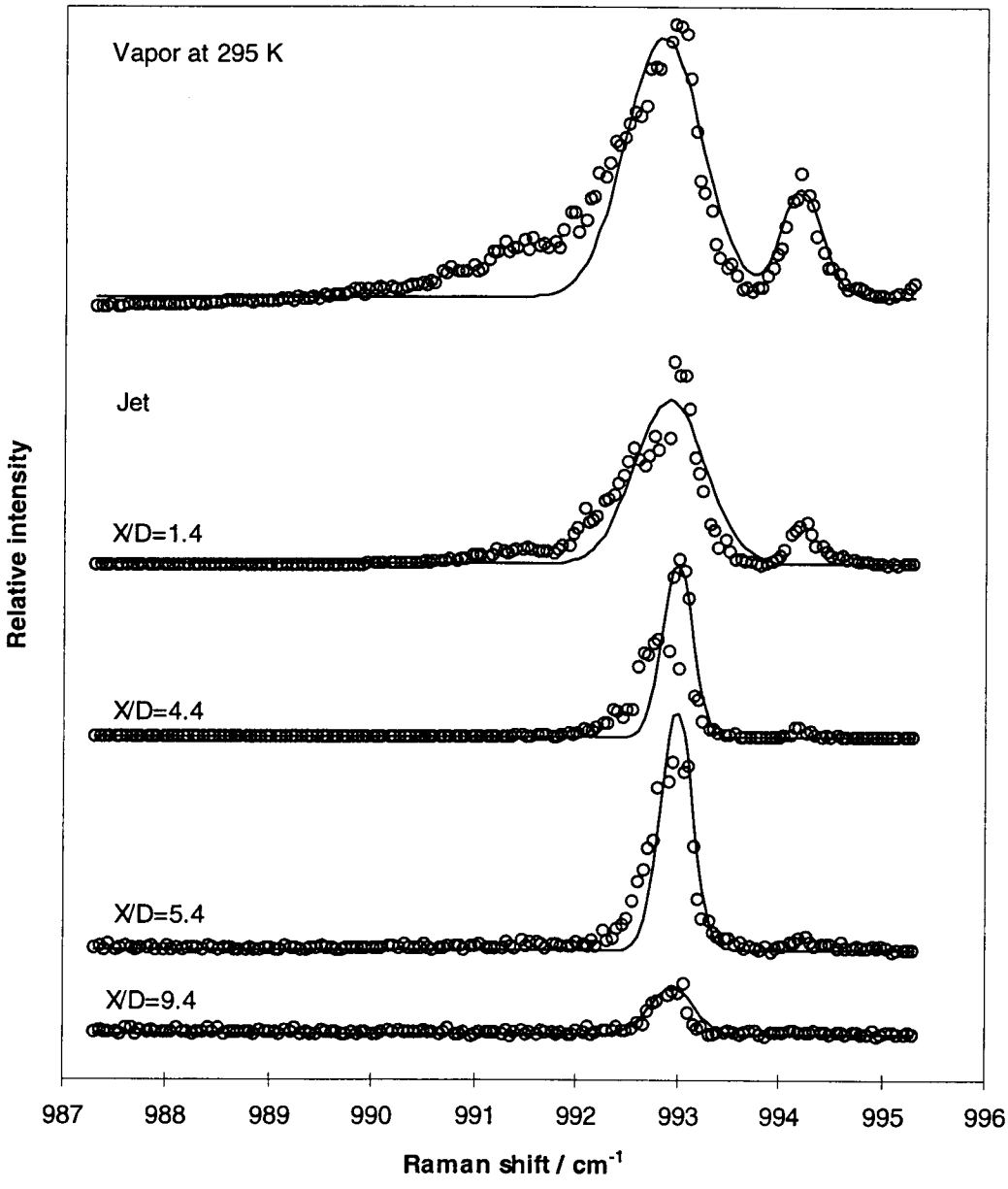

Figure 5-1. CARS spectra of pure benzene vapor in jet expansions with the large nozzle. The benzene was at room temperature where it has a vapor pressure 82 torr. The nozzle temperature was at around 42 C.

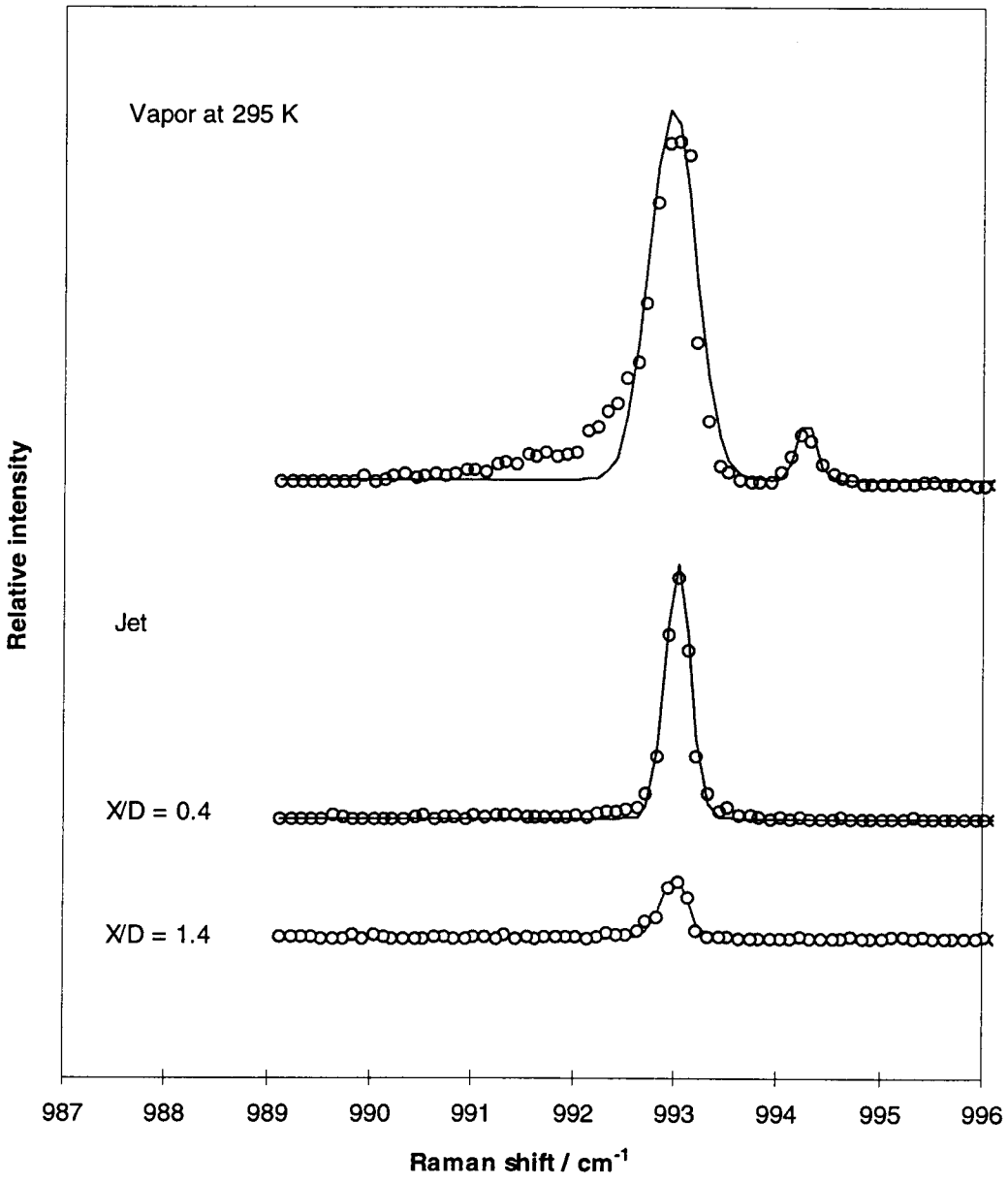

Figure 5-2. CARS spectra of neat benzene vapor in jet expansions with the small nozzle (D =0.5 mm). The benzene was at 62 C where it has a vapor pressure of 416 torr. The nozzle temperature was at 65 C.

Table 5-1. Jet experiment of neat benzene vapor at room temperature for a large nozzle. June 23, 1996 data.

X/D D=0.5	shift[a] cm^{-1}	STD error	FWHM cm^{-1}	STD error	Peak area
Vapor	992.834	0.018	1.264	0.027	42.44
1.4	992.978	0.012	0.695	0.017	7.83
2.4	993.026	0.009	0.507	0.013	7.59
3.4	993.033	0.006	0.419	0.009	2.58
4.4	993.061	0.005	0.302	0.008	1.88
5.4	993.057	0.004	0.316	0.006	2.71
6.4	993.033	0.005	0.305	0.007	3.49
9.4	993.022	0.014	0.428	0.020	0.71

a) Calibrated shift of 3.57 cm^{-1} was used

Table 5-2. Jet experiment of neat benzene vapor at 62 C for a small nozzle. May 22 1996 data.

X/D D=0.25	shift[a] cm^{-1}	STD error	FWHM cm^{-1}	STD Error	Peak
Vapor	992.978	0.009	0.458	0.027	4.29
Vapor	992.956	0.011	0.440	0.017	1.63
0.4	993.043	0.002	0.250	0.003	1.63
1.4	993.017	0.005	0.256	0.007	0.41

a) Calibrated shift of 2.84 cm^{-1} was used

5.3.2. Helium driven benzene for a large nozzle

When we mix benzene vapor with helium, the mixture has a much higher total pressure than pure vapor benzene and greater cooling is expected. At helium driving pressures of 3.4 and 4.7 atm and benzene vapor at 295 K, clusters are readily formed in jet expansions, as seen in Figure 5-3 and Figure 5-4. The vapor peak is always present in the spectra at different X/D positions. The Raman shift of the cluster peak is plotted in Figure 5-5 and the temperature deduced from equation 4.1 (assuming the cluster is liquid) is shown on the axis to the right and is listed in Table 5-3. By comparison to the Raman-temperature relation of the bulk phase (Figure 4-8), these Raman shifts of clusters (991.2 to 991.6 cm^{-1}) are lower than liquid but higher than solid. It is clear that no solid clusters were formed in the jet with the large nozzle (D = 0.5 mm). All the clusters were supercooled liquid.

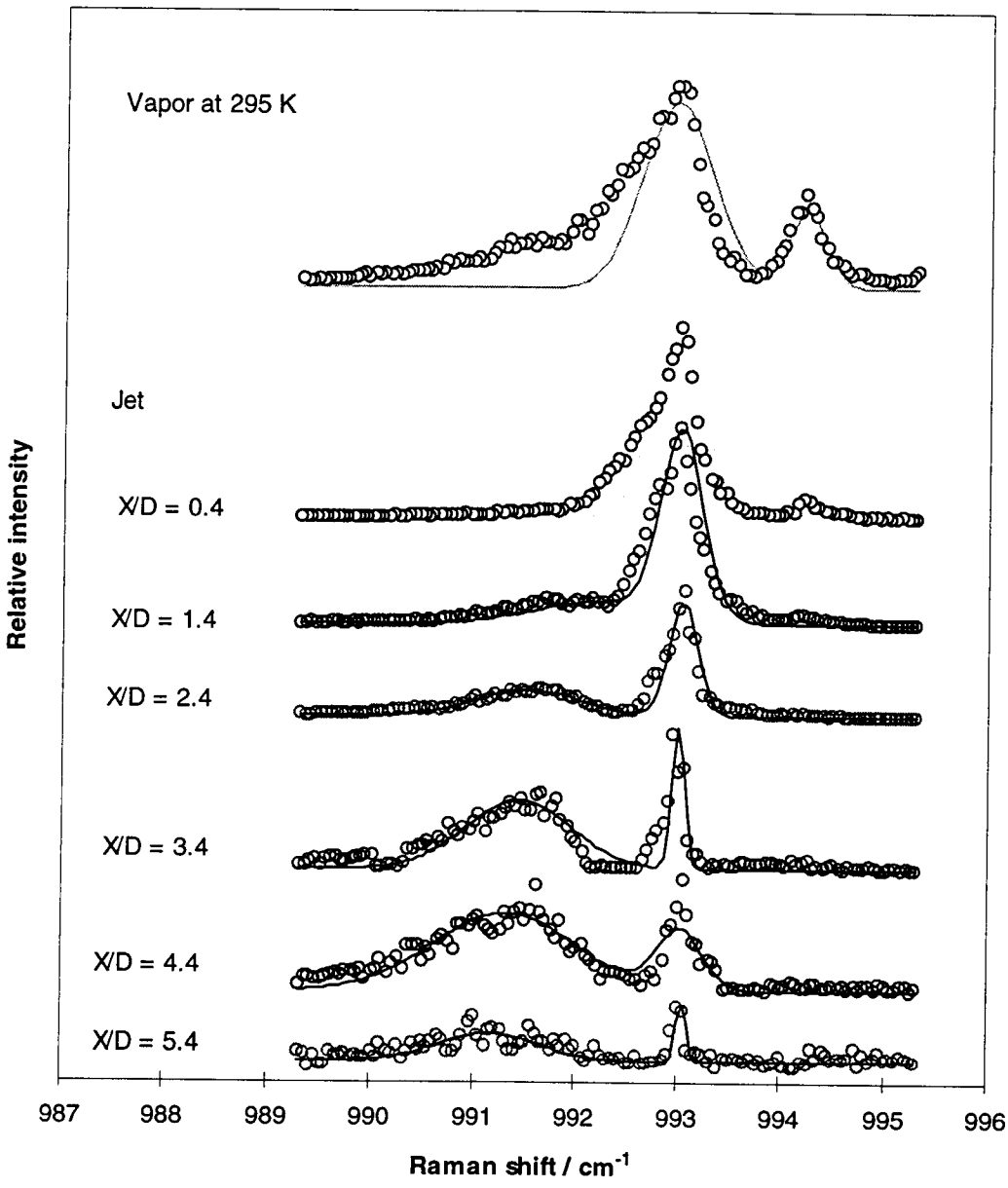

Figure 5-3. CARS spectra of benzene in jet expansions with the large nozzle. The circles are experimental data, the solid lines are peakfitting curves. The benzene was at room temperature where it has a vapor pressure 82 torr. The helium driving presure was at 3.4 atm. The mole ratio of benzene is 3.2% . The nozzle was at 42 C .

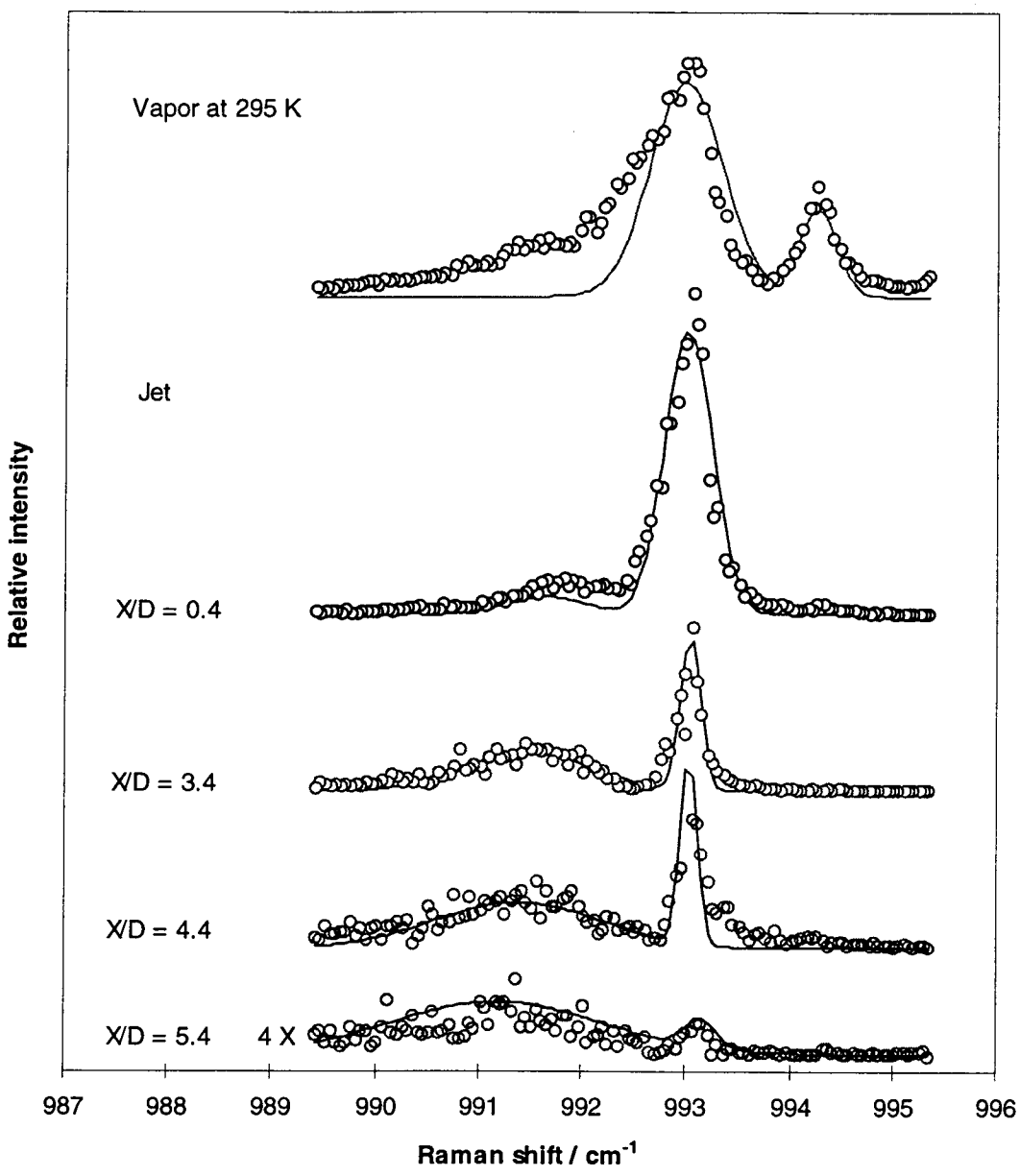

Figure 5-4. CARS spectra of benzene in jet expansion with the large nozzle. The circles are experimental data, the solid lines are peak fitting curves. The benzene was at 295 K where it has a vapor pressure of 82 torr. The helium driving pressure was at 4.7 atm. The mole ratio of benzene is 2.3% . The nozzle was at 42 C .

Table 5-3. Helium driven benzene in a large nozzle. June 23, 1996 data.

	Monomer				Cluster				
X/D D=0.5	shift[a] cm^{-1}	STD error	FWHM cm^{-1}	Peak area	shift[a] cm^{-1}	STD error	T[b] K	FWHM cm^{-1}	Peak area
3.4 atm									
0.4	992.991	0.006	0.51	4.4					
1.4	993.040	0.005	0.42	3.8	992.270	0.136	299.1	1.34	1.4
2.4	993.076	0.004	0.29	1.6	991.539	0.032	267.1	1.02	1.2
3.4	993.025	0.004	0.12	0.9	991.460	0.023	263.6	1.01	3.2
4.4	993.052	0.023	0.45	1.3	991.328	0.032	257.8	1.38	4.6
5.4	993.075	0.007	0.09	0.1	991.181	0.047	251.4	1.27	0.8
4.7 atm									
0.4	993.011	0.005	0.46	5.5	991.634	0.115	271.2	0.75	0.5
3.4	993.041	0.003	0.19	1.3	991.455	0.057	263.4	1.22	1.9
4.4	993.026	0.004	0.16	1.3	991.366	0.054	259.5	1.60	2.7
5.4	993.100	0.008	0.19	0.2	991.248	0.064	254.3	1.29	0.4

a) Calibrated shift of 3.55 cm^{-1} was used

b) The temperature is deduced assuming the cluster is supercooled liquid

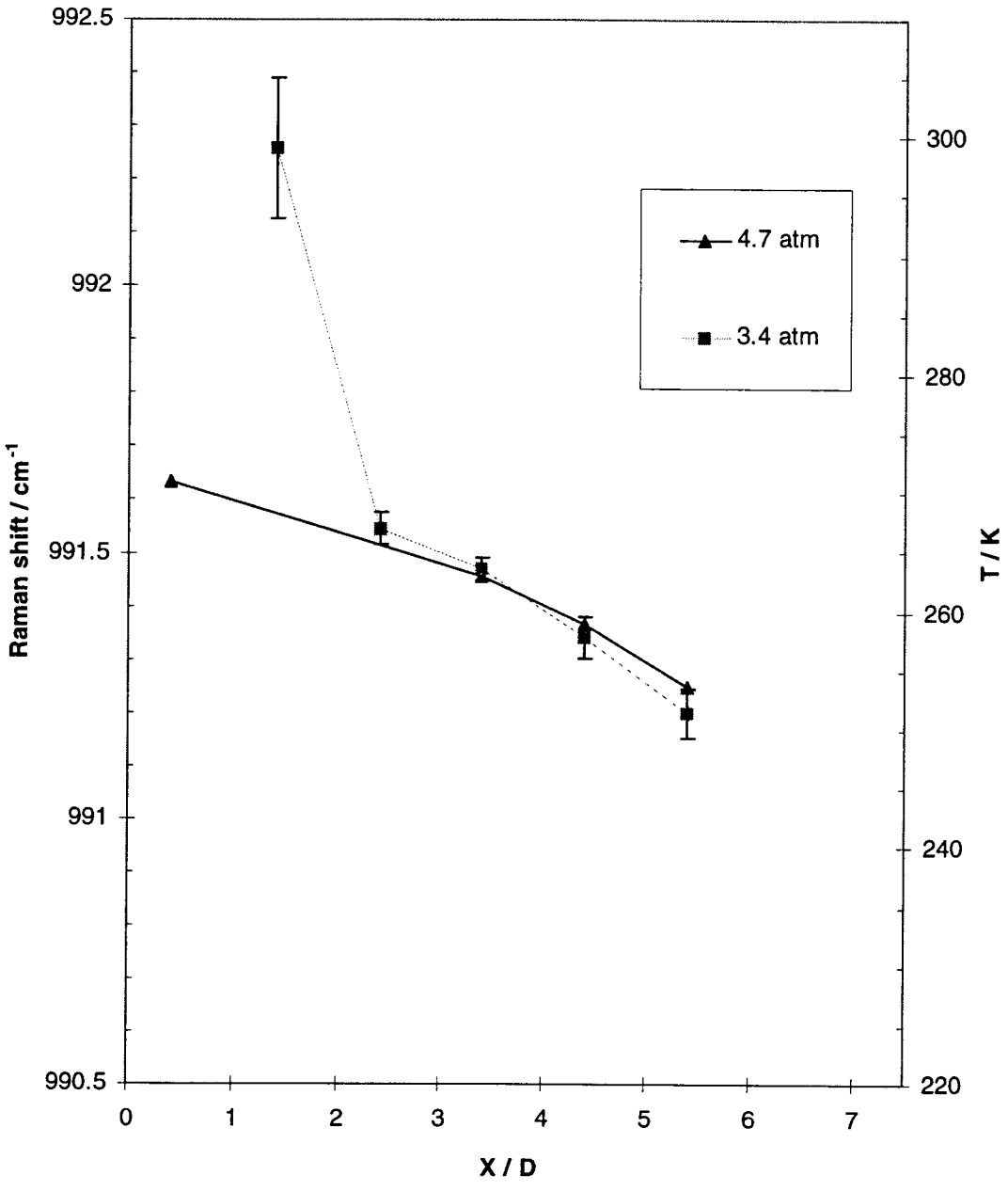

Figure 5-5. Raman shift of clusters in the large nozzle jet expansion. The benzene was at 295 k where it has a vapor pressure of 82 torr. The helium driving pressures were 3.4 or 4.7 atm, corresponding to mole ratios of 3.2% or 2.3%. The nozzle was at 42 C.

5.3.3. Helium driven benzene in a small nozzle

From the pure benzene vapor jet experiments, we expect that benzene will be cooled more for expansions with the smaller diameter nozzle (D = 0.25 mm). This is borne out in Figure 5-6, 5-8 and 5-9 that show spectra for the latter case for helium driven expansions. We see that the monomer peak quickly disappears as X/D increases, compared to the large nozzle (D = 0.5 mm) expansion, indicating that the colder molecular beam results in more extensive clustering. However there is still only one broad cluster peak seen in the spectra. The Raman shifts versus helium driving pressure at the first two fixed X/D positions are plotted on Figure 5-10, which shows that the Raman shifts increase with increasing helium driving pressure and then level off. The shifts are all smaller than expected for solid; comparison with Figure 4-8 shows that all the clusters are supercooled liquid. The temperatures are shown on the right axis. The Raman shifts of this cluster feature versus X/D are plotted in Figure 5-7 and 5-11 and the temperatures deduced assuming that the clusters are liquid are shown on the secondary axis. Note that none of the cluster Raman shifts are sufficient to reach those of solid benzene, which is below 990.55 cm^{-1}. Interestingly, the shifts decrease slightly at larger X/D positions, indicating that warming has occurred. We also see that the higher the driving pressure, the sooner this warming happens (Figure 5-11). These decreases of Raman shift indicate that the clusters began to warm instead of cooling as they traveled downstream from the nozzle.

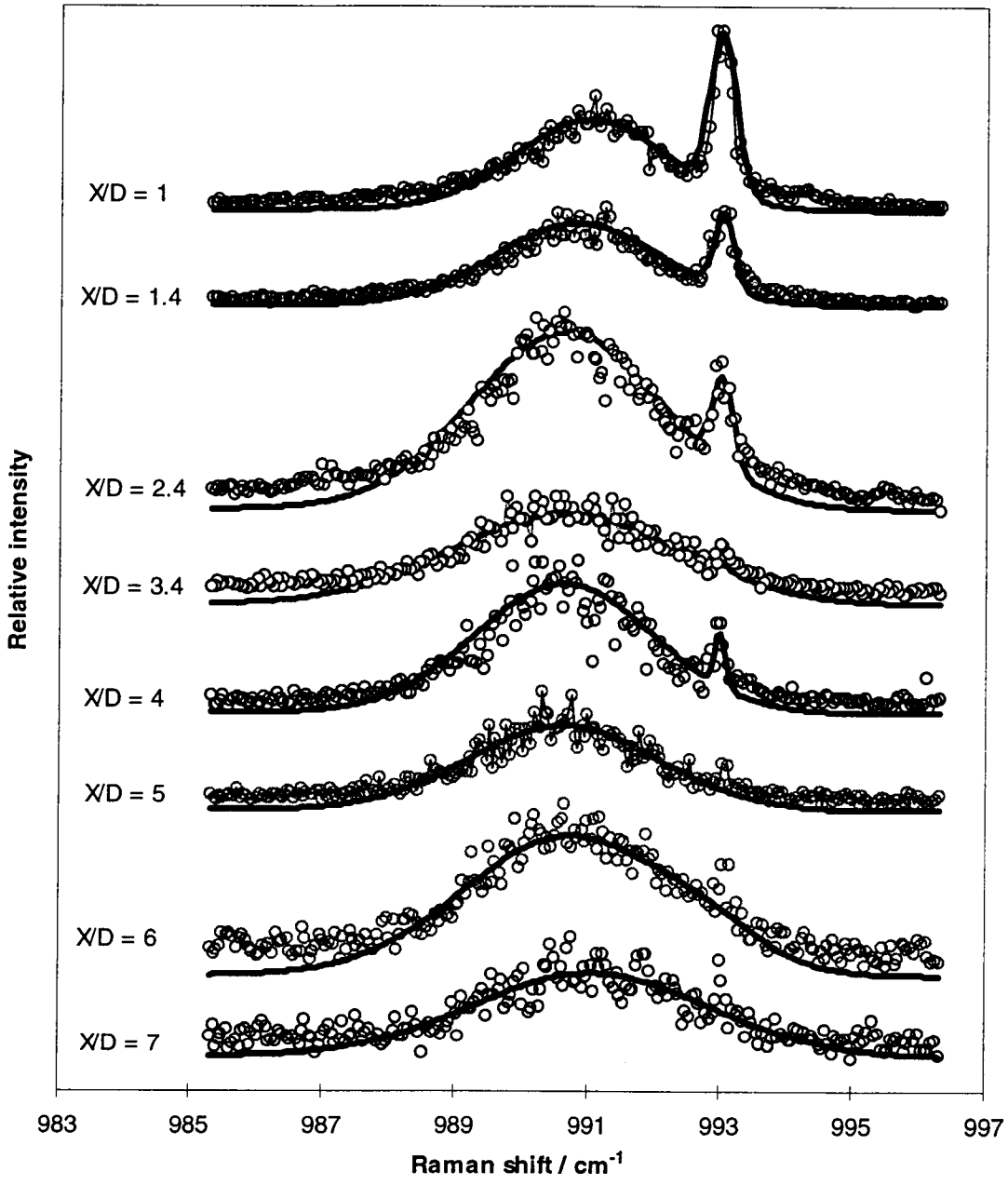

Figure 5-6. CARS spectra of benzene in jet expansion of Sept. 6, 1995. The helium driving pressure was 4.4 atm and the benzene was at 295 K. The benzene mole ratio is 2.5 %. The nozzle was at 42 C.

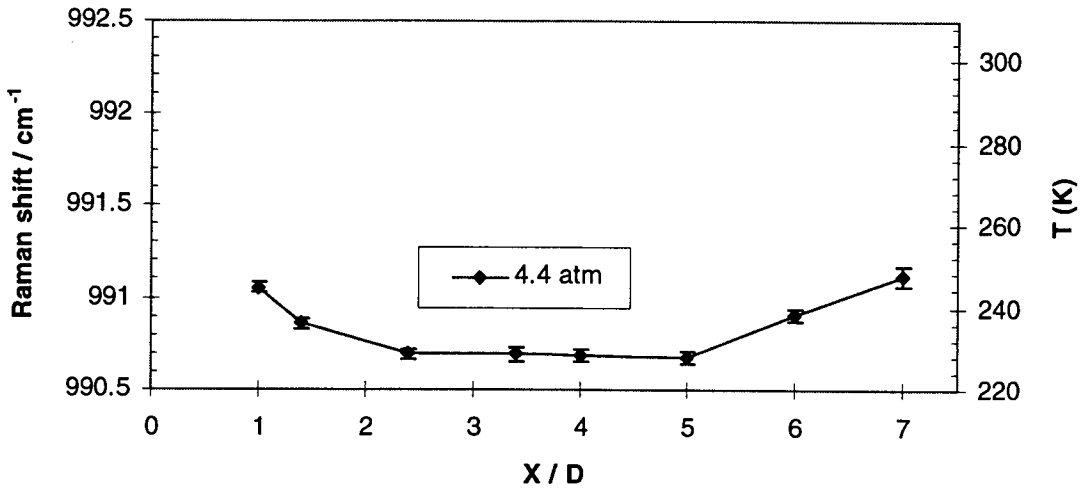

Figure 5-7. Raman shift versus X/D in the small nozzle (D=0.25 mm) jet expansion. Sept 6, 1995 data.

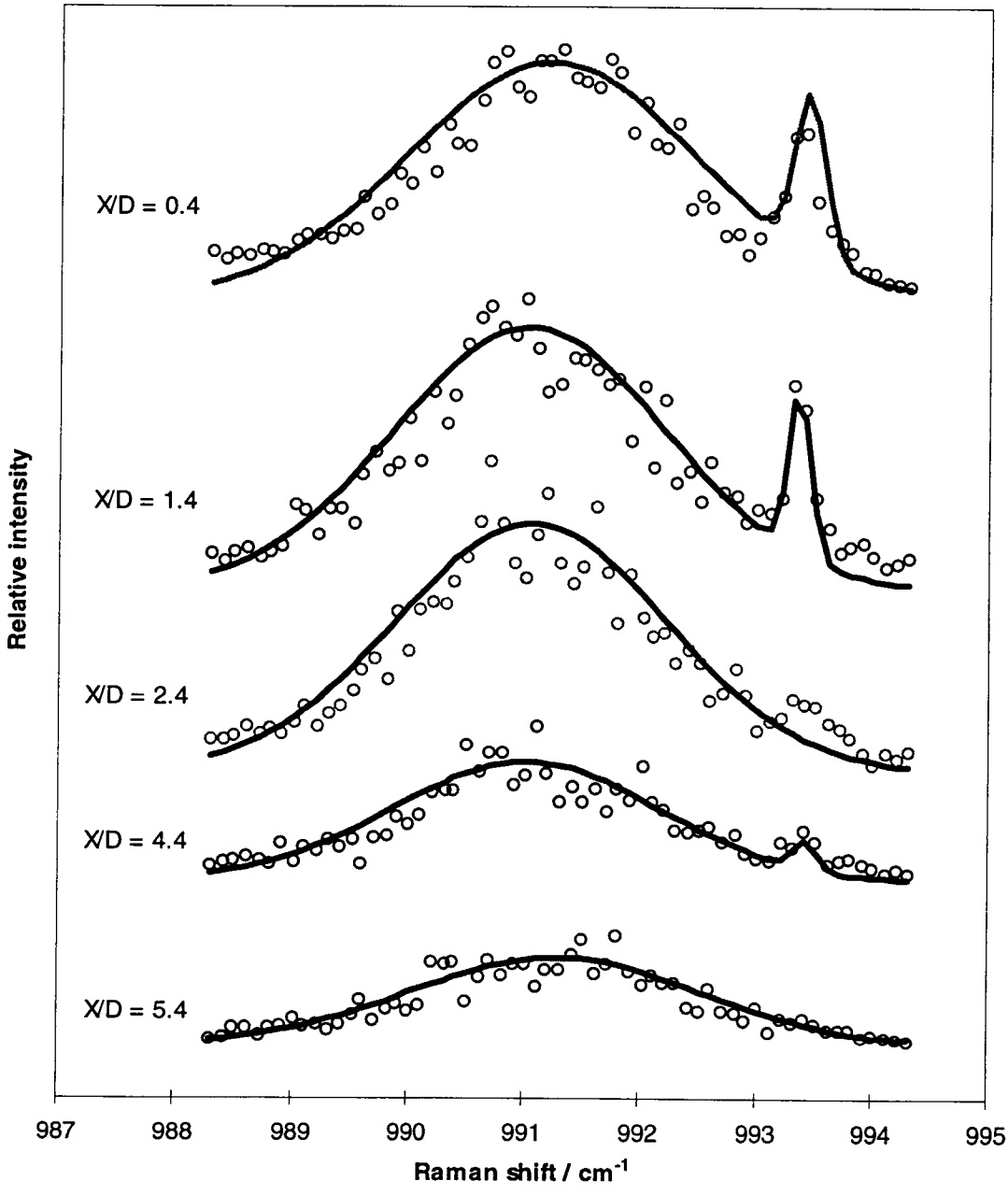

Figure 5-8. CARS spectra of benzene driven with 3.4 atm helium in the small nozzle jet. The nozzle temperature was around 42 C. The benzene mole ratio is 3.2%.

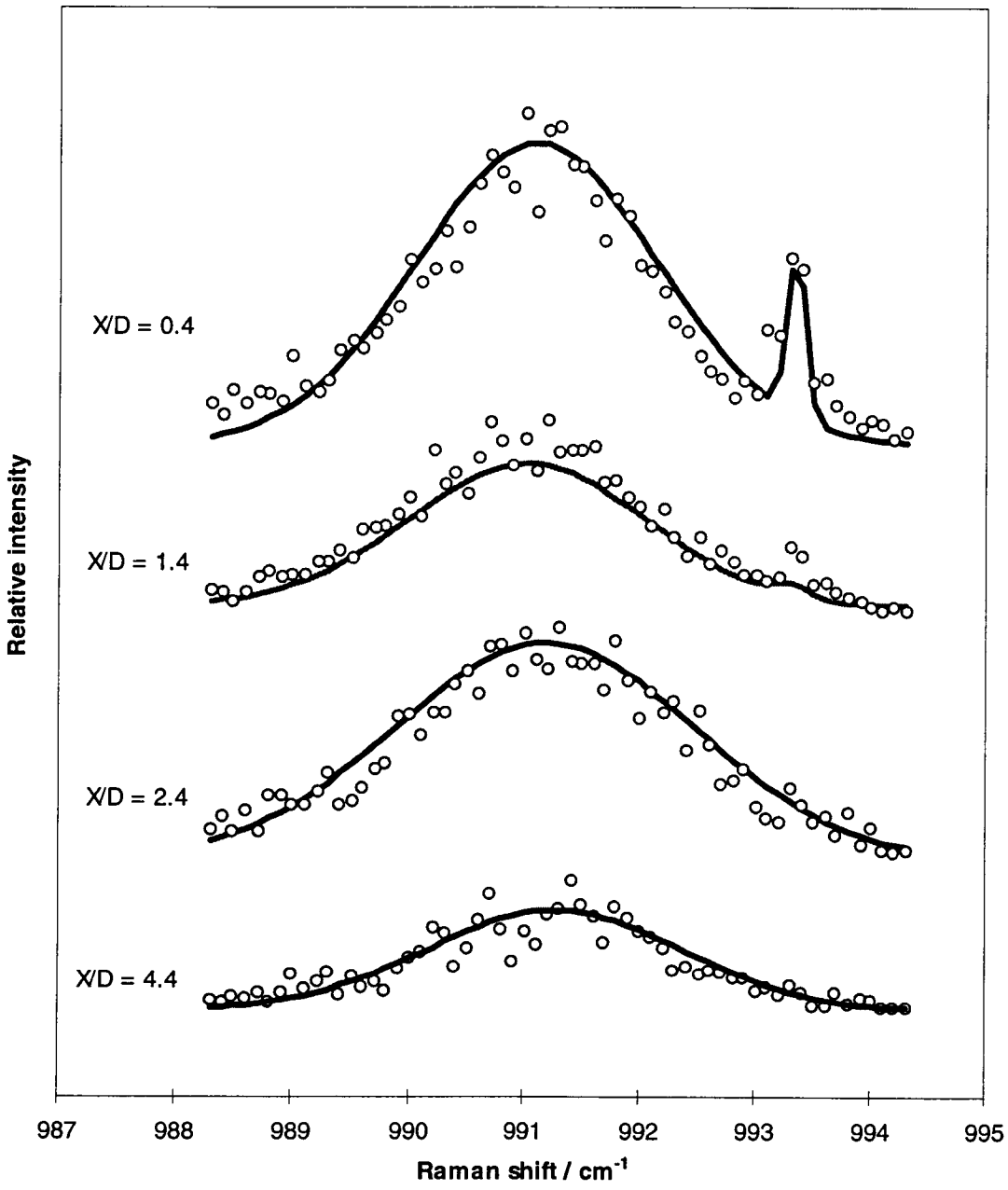

Figure 5-9. CARS spectra of benzene driven with 4.7 atm helium in the small nozzle jet. The nozzle temperature was around 42 C. The benzene mole ratio is 2.3%.

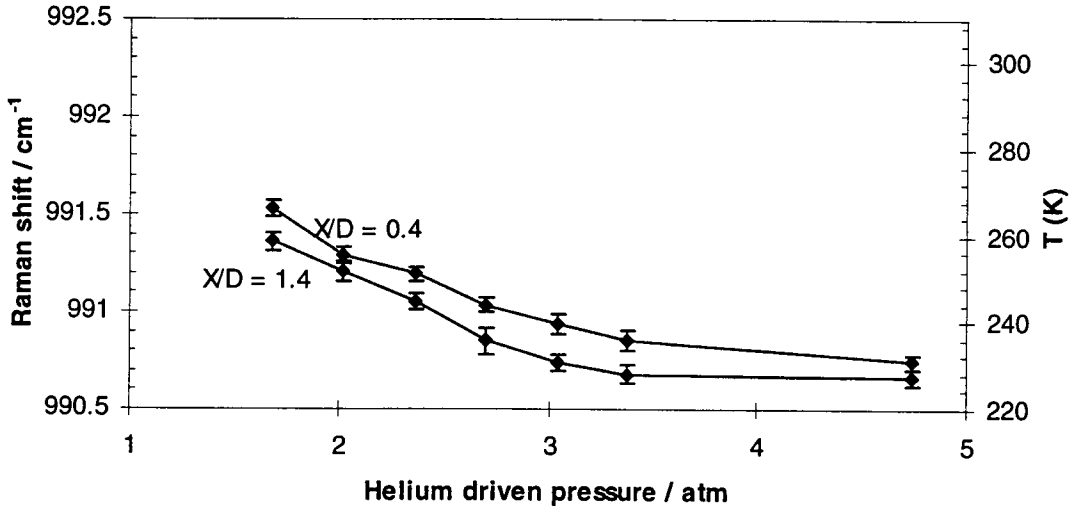

Figure 5-10. Raman shift of benzene clusters in the jet versus helium driving pressure.

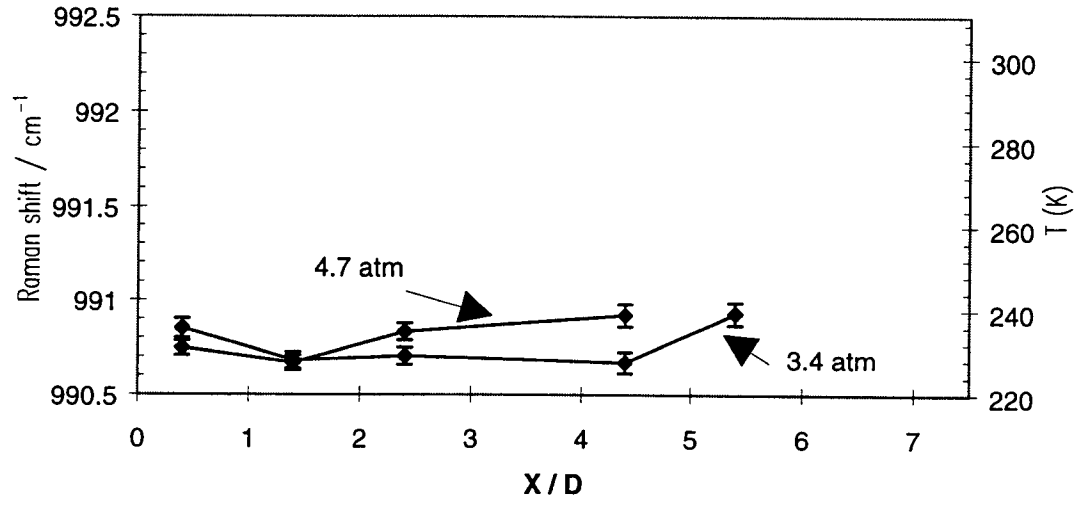

Figure 5-11. Raman shift of benzene clusters in the jet with the small nozzle (May 21, 1996 data).

These trends do not agree with our expectation that "the larger X/D, the colder the molecular beam" and "the higher the driving pressure, the colder the molecular beam". What caused the temperature rise? One might suspect Mach disc warming, as was seen in the neat benzene expansion discussed in section 5.3.1. However, this is not viewed as likely in the present case because for 3.4 and 4.7 atm driving pressures the Mach disc is calculated to be located at 34 and 40 X/D units respectively, distances far beyond our probing region (less than 8 X/D). Another reason might be the heat of condensation if vapor molecules collide with clusters which are continuing to grow in size. If this is true, we should have seen the same warming effect due to condensation in the larger diameter nozzle jet experiments. Examining Figure 5-6, 5-8 and 5-9, we see that the extent of clustering in the small nozzle (D = 0.25 mm) case is greater, and indeed, clustering is essentially complete; hence no further warming due to condensation would be expected.

There remains only the possibility that the clusters supercool in the jet to the point that some freezing into solid occurs. When the phase transition from liquid to solid happens, the heat of fusion being released would certainly cause warming of the clusters. This would explain our observation of a Raman shift decrease at higher X/D locations, and higher driving pressures, see Figure 5-7 and 5-11. Thus we believe that the observation of the Raman shift decrease serves as an indicator for the onset of a liquid-solid phase transition, even though separate features for the two phases can not be distinguished.

5.3.4. Reliability of Raman shift measurements determined by CARS

In all the spectra in the jet experiments, the cluster peaks have considerable noise and it is necessary to ask how reliable and accurate is the peak position information derived from these spectra? Statistical error analysis gives a minimum uncertainty, which is shown as error bars in the figures. We note that the peak position and uncertainties were essentially the same for assumed Gaussian or Lorentzian shapes. The relatively smooth variation in position from point to point (see Table 5-4 and 5-5) suggests that the relative accuracy of the peak position, and hence the temperature change, is reasonably consistent with the error bars shown in the figures. However the absolute shifts and temperatures have a much larger uncertainty, which we estimate could be as high as $\pm$ 0.1 cm^{-1}, corresponding to about $\pm$ 5 K absolute temperature uncertainty.

5.4. Model of Supercooling and Freezing Processes

In the above discussion, we suggest that liquid clusters form, supercool, and then, at a certain lower temperature T_L, begin to freeze into solid. The solid formed must warm to the melting point due to the heat of fusion. Thus at this onset of freezing, the sample must consist of mostly supercooled liquid clusters at T_L plus a small fraction of clusters in which liquid and solid coexist at T_m = 278.4 K. The latter clusters would contribute two peaks to the spectrum, at Raman shifts of 991.80 (liquid) and 990.56 (solid) cm^{-1} respectively. These would not be resolved from the supercooled liquid

Table 5-4. Sept 6,1995 jet experiment data summary.

	Monomer				Cluster				
X/D D=0.25	shift[a] cm^{-1}	STD error	FWHM cm^{-1}	Peak area	shift[a] cm^{-1}	STD error	T^b K	FWHM cm^{-1}	Peak area
4.4 atm									
1.0	993.059	0.004	0.300	2.7	991.053	0.022	245.8	2.33	10.5
1.4	993.083	0.008	0.335	1.4	990.859	0.020	237.3	2.55	10.3
2.4	993.070	0.012	0.321	1.6	990.693	0.019	230.0	2.90	24.8
3.4	992.928	0.107	0.450	0.2	990.696	0.034	230.1	3.46	14.5
4.0	993.048	0.016	0.194	0.4	990.687	0.027	229.8	2.70	17.1
5.0					990.681	0.028	229.5	2.88	11.8
6.0					990.905	0.030	239.3	3.70	24.5
7.0					991.112	0.051	248.4	3.61	14.0

a) Calibrated shift of 2.56 cm^{-1} was used

b) The temperature is deduced assuming the cluster is supercooled liquid

Table 5-5. May 21,1996 jet experiment data summary.

	Monomer				Cluster				
X/D D=0.25	F cm^{-1}	STD error	FWHM cm^{-1}	Peak area	F cm^{-1}	STD error	T^b K	FWHM cm^{-1}	Peak area
3.4 atm									
0.4	993.080	0.021	0.269	1.7	990.852	0.043	237.0	2.48	18.9
1.4	993.005	0.013	0.192	1.4	990.682	0.035	229.5	2.35	20.3
2.4					990.704	0.037	230.5	2.34	19.1
4.4	993.065	0.070	0.203	0.2	990.670	0.048	229.0	2.30	9.1
5.4					990.931	0.054	240.4	2.51	7.1
4.7 atm									
0.4	992.997	0.012	0.16	0.9	990.746	0.027	232.3	2.10	17.9
1.4	993.007	0.018	0.07	0.2	990.669	0.030	228.9	2.43	12.0
2.4					990.833	0.036	236.2	2.61	15.0
4.4					990.922	0.053	240.0	2.23	6.3

a) Calibrated shift of 2.65 cm^{-1} was used

b) The temperature is deduced assuming the cluster is supercooled liquid

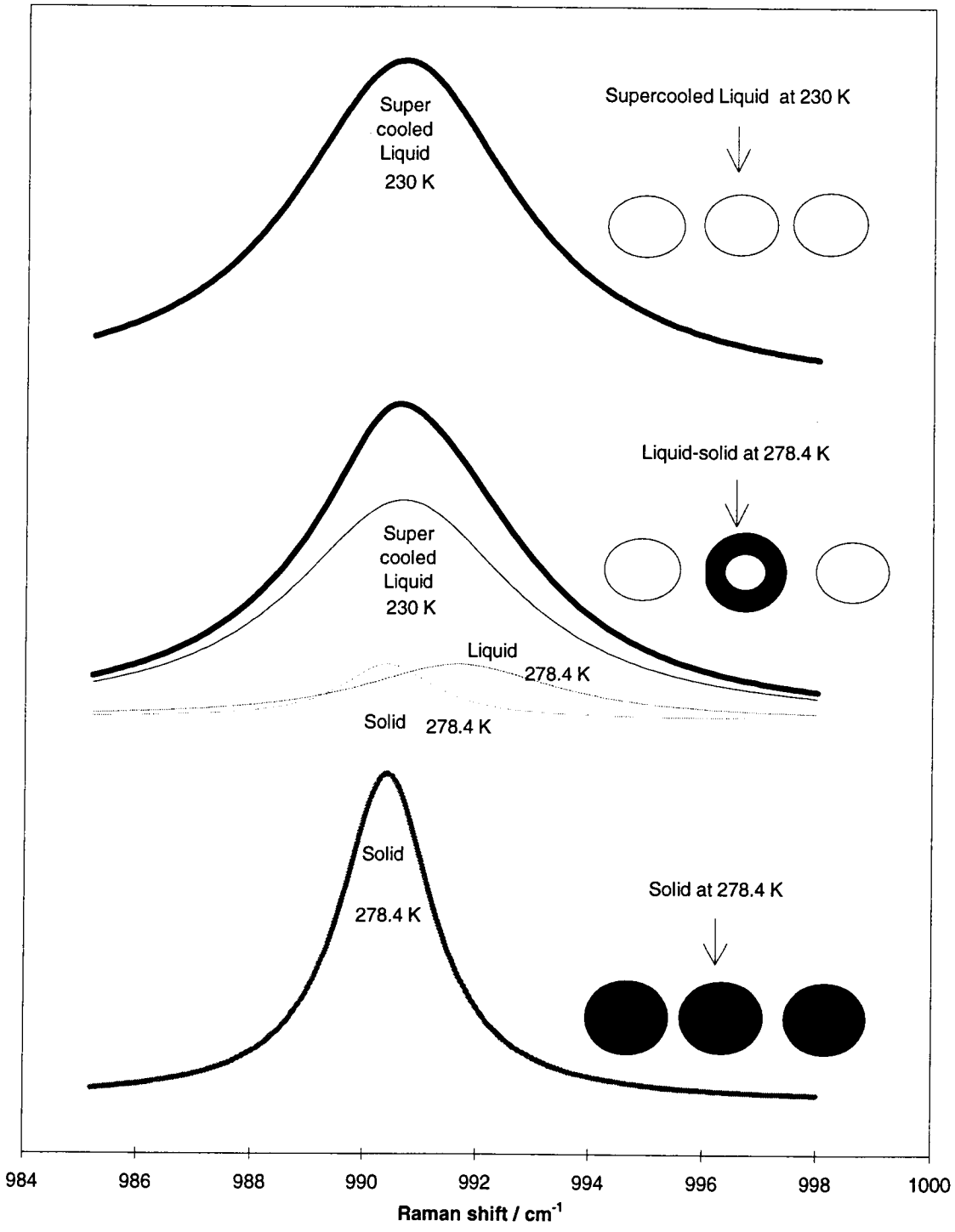

Figure 5-12. Model of spectral changes expected for freezing process

feature but would cause an overall broadening of the peak, as observed in Figure 5-6, 5-8 and 5-9. Since the change in peak position is greater for the liquid fraction of the mixed clusters, compared to that of the solid, an overall shift of the peak to a higher wavenumber value is predicted, as observed. Eventually, of course, all of the supercooled liquid clusters would freeze and the jet spectra should show only a single, relatively sharp feature centered at the solid value at 278.4 K. The sequence of these events is depicted in Figure 5-12. It is clear that total freezing does not happen in the X/D range that we are able to probe with the sensitivity of our apparatus. Thus we can only conclude that some partial freezing of the liquid cluster is occurring in our experiments.

Researchers have examined benzene clusters of varied sizes by different methods for over a decade.[42,54,83] It is noteworthy that our experiments indicate the formation of solid clusters since benzene is known to be difficult to freeze in a jet.[18] Aggregates less than 27 units of benzene were found only in liquid state in the jet.[42] Large clusters of 20 nm diameter were observed only in a liquid form in the jet.[11,84] In general, it was found that more complex polyatomic molecules apparently form liquid clusters easily.[85] Efforts to understand this observation were conducted mainly through Monte Carlo theoretical simulation.[86] Benzene, as a representative molecule, has been investigated with Monte Carlo carefully.[87-89] The molecular structure (aspherical shape) and kinetics reasons (benzene needs over 100 μs to freeze , which is out of jet probing range) have been proposed for the observation of only liquid clusters in the jet.[85] However, mass spectra evidence does indicates co-existence of liquid and solid phases for a very small aggregates (13 unit),[90] and solid features for aggregates of less

than 20 benzene unit.[83] Our clusters are believed to be of the order of 10 nm in size, similar to those produced in the electron diffraction experiments, and no evidence was seen of very small liquid or solid aggregates.

Our results shows that clusters of solid benzene can be prepared and detected in the jet. It is difficult to form solid clusters in the jet for polyatomic molecules, such as benzene, the reason is the larger heat of condensation compared to that of small molecules. The jet needs to remove this heat of condensation before it could be further cooled down to freeze. This explanation can be justified with our spectra, see Figure 5-6, 5-8 and 5-9, which show clusters freeze after monomer has been depleted.

5.5. Determination of Interfacial Tension σ_{sl} of Solid from Jet Experiments

5.5.1. Introduction

Surface tension σ_{lv} is an important fundamental physical property which is compiled in most physical chemistry data references. However, no information has been available for surface tension of solids σ_{sv} or of solid-liquid interfacial tensions σ_{sl} in those books. Even in research papers, very few data exist for σ_{sv} or σ_{sl} of solids and most of this is for metals, not for molecules.[5] Different methods have been used to measure these values for metals, including calorimetry,[91]heat of solution,[92] and others that give a relative error range from 30% to 80%. Field emission microscope,[93] foil and wire zero creep[94,95] and contact angle experiments[96] give a relative error ranges 10% to

20%. The most accurate method is compensated creep wire or foil,[97] which claims an uncertainty range of 1% to 3%.

The above methods have been used for the measurement of surface tension of metals, but are not generally applicable for other materials, such as organic molecules. In chapter 2, we noted that interfacial free energy of solid can be determined from homogeneous nucleation theory if we can measure the rate of nucleation and know other physical properties. Here we discuss in detail how to determine the rate of freezing from equation (2.11) and σ_{sl} from the homogeneous nucleation equation (2.8). For the convenience of discussion, we reproduce these equations below.

$$J = [2(\sigma_{sl}k_bT)^{1/2}/(v_m^{5/3}\eta)] \exp(-16\pi\sigma_{sl}^3/(3\Delta G_v^2)k_bT) \qquad (2.8)$$

$$F_s = 1-\exp(-Jvt) \qquad (2.11)$$

In the following sections, we consider the determination or estimate of various quantities in these equations and then use these deduced value to calculate σ_{sl} for benzene.

5.5.2. Estimate of the mean size of clusters in the jet

The volume (v) of the clusters has to be determined for the calculation of the rate of nucleation via equation (2.12). There are several ways which have been used in our lab to estimate the mean size of such clusters. The first involves the modeling of cooling of clusters as functions of X/D in the supersonic jet experiment.[14] This cooling

curve model is not helpful in our experiments for benzene because we do not have a single liquid or solid cluster peak to use to deduce temperature. A second method has been used when the cluster is small and there are spectral features that can be assigned to molecules on the surface.[98] In this case, the ratio of the surface to bulk molecules can give a good estimate of the size of clusters. Unfortunately, no such surface feature is seen in our jet experiments on benzene. A third method, recently developed by Steve Mayer,[99] involves Rayleigh scattering[100,101] As it happens, this development came after the completion of my experiments and thus no direct measurement of cluster size was done in my experiments.

Fortunately, since the size of cluster has only a small effect on the σ_{sl} values,[9,10] we can make an adequate estimate of the size of benzene clusters in our experiments from these other studies which used similar expansion conditions. In particular, in our lab the diameters of clusters for other molecules determined by cooling curve, Rayleigh scattering, and surface to bulk core ratio methods have all been in the range from 5 to 50 nm. For example, a 12% CO_2 mix with 14 atm helium produced an estimated mean cluster diameter of 14 nm, while under similar conditions a 5% CO_2 expansion produced clusters with a mean diameter of 8 nm.[99] In his study of benzene clusters formed in jets,[12] Bartell's simulation led to a cluster diameter of 20 nm for a jet with a Laval nozzle (entrance diameter 0.128 mm, exit diameter 1.9 mm, length 30 mm). The helium driving pressure ranged from 0.5 to 2.2 atm, giving a molar ratio of benzene from 0.01 to 0.2. The Laval nozzle generally produces larger clusters than does our shim (sonic) type of nozzle. In our experiments, the helium driving pressure was 3.4

and 4.7 atm, giving mole ratios of 0.0022 and 0.0015 respectively. All of our experimental conditions suggest that the size of benzene clusters in our jet experiments should be smaller than those in Bartell's experiments. Accordingly, we believe a reasonable estimate is a mean diameter of 10 nm.

5.5.3. Determination of the rate of nucleation

In the following we assume that the rate of nucleation J can be equated to the observed rate of freezing; justification for this comes from the experiments of Minarik.[28] The rate of freezing can be obtained from equation (2.11) if we can estimate the duration (t) of freezing of some specified fraction of the liquid clusters in the jet. We will assume that, at most, 50% of the clusters will have frozen in our experiments since a larger fraction would be expected to result in the appearance of a solid feature in the spectra. We obtain an upper limit on the rate of nucleation by assuming that this extent of freezing occurs in two X/D units, as suggested by Figure 5-7 and 5-11. The velocity of the benzene clusters can be deduced from the isentropic expansion relations,[13,102] giving a value of about 1400 m s^{-1} for our experimental conditions (2.5 % benzene mole ratio, X/D = 5 to 7 and total helium driving pressure P_0 = 4.4 atm). Thus the duration (t) is 0.36 μs. For an assumed mean cluster diameter of 10 nm, the volume (v) is 5.2×10^{-25} m^3. These values give J = 3.7×10^{30} m^{-3} s^{-1} for benzene, a value believed to be good to about ± one order of magnitude.

5.5.4. Determination of temperature of freezing

To calculate σ_{sl} from equation (2.8), we need to know the nucleation temperature T_L at which freezing happens. If we assume that the data of the liquid Raman shift we measured in bulk sample can be linearly extrapolated to the supercooled liquid region, the measured Raman peak in the region of freezing yields, via equation (4.1), $T_L = 230$ K.

5.5.5. Determination of other physical parameters in equation (2.8)

Other parameters in equation (2.8) need to be estimated at the nucleation temperature T_L. For viscosity, equation (2.9) is used to extrapolate the available experimental data of liquid[44] to the supercooled region. Data for the heat capacity of solid and liquid[58] are used to calculate the variation of entropy change with temperature. Linear extrapolation is used to estimate the heat capacity in the supercooled region for liquid benzene. A summary of all relevant parameters is given in Table 5-6.

5.5.6. Determination of σ_{sl} and estimate of uncertainty

With the above determined values of the rate of nucleation J, the temperature of nucleation, and the viscosity equation (2.8) yields a value of 11.7 mJ m^{-2} for σ_{sl}. The uncertainties in nucleation rate and cluster size will manifest themselves in J; we find that a change of J by a factor of $\pm$ 100 produces only a $\pm$ 10% change in σ_{sl}. This is

Table 5-6. Summary of all relevant parameters in equation (2.8)

Parameters	Value		Unit	Data source
Melting point T_m	278.4		K	CRC 77th [d]
Heat of fusion H_{fus}	9950		J/mol	CRC 77th [d]
Molar volume of liquid V	89.04		m^3/mol	CRC 77th [d]
Boltzmann constant K	1.38066E-23			CRC 77th [d]
Avogandro constant N_a	6.023E+23			CRC 77th [d]
Molecular weight W	78.05		g/mol	CRC 77th [d]
Density of liquid (l)	0.8765		g/cm^3	CRC 77th [d]
Density of solid (s)	1.016		g/cm^3	CRC 77th [d]
Molecular volume V_m	1.27541E-22		m^3/molecule	CRC 77th [d]
Heat capacity of liquid (295 K) Cp(l)	136.00		J mol^{-1} K^{-1}	CRC 77th [d]
Fusion entropy at 278.4 K DS_{fus}	173.40		J mol^{-1} K^{-1}	CRC 77th [d]
	a	b	c	
[a] Cp(l) fitting coefficients	68.04756	0.22858		Oliver [e]
[b] Cp(s) fitting coefficients	44.1415	-0.06232	0.00131	Oliver [e]
	A	B	T_0	
[c] Viscosity fitting coefficients	-1.4441	243.1342	99.7165	CRC 50th [f]
Nucleation temperature T	230		K	
Del G_v (230 K)	19185318.10		J/mol	
Viscosity (230 K)	2.64		mPasc S	
Sigma liquid-solid (230 K)	11.7		mJ m^{-2}	

a) $Cp(l) = a+b*T$

b) $Cp(s) = a+b*T+c*T^2$

c) $\log \eta = A+B/(T-T_0)$

d) CRC 77th, 1997.[103]

e) Oliver, 1948.[58]

f) CRC 50th, 1970.[57]

illustrated in Table 5-7, where the effect of a ±10 K change in cluster temperature is also examined.

5.5.7. Discussion

From the above considerations, we obtain a lower limit of 11.7 mJ m^{-2} for σ_{sl} for benzene at 230 K. There is only one other value for benzene available for comparison. Staveley[10] used the same nucleation theory and cloud chamber measurements to deduce a rate of freezing 1.5 x10^{12} m^{-3} s^{-1} and a value 20.4 mJ m^{-2} at 208 K. Stavely's value is substantially greater than our result, more than might be expected for his colder sample. There is however some concern that Staveley's experiments tend to underestimate the rate of nucleation[32] because the time period for the liquid drop to cool to the nucleation temperature T_L was also included in the nucleation time. He equated the overall cooling period (seconds to minutes in his experiments) to the nucleation rate. However, as we discovered in our experiments, and as seen in other published work,[13,14,19]this can occur within microseconds. Such a large increase in nucleation rate would decrease his value of σ_{sl} substantially so his value of 20.4 mJ m^{-2} should be considered as an upper limit.

Another comparison can be made with Turnbull's empirical equation (1.1), which is based mainly on results from experiments on metals and a few organic molecules. Turnbull's equation predicts a value of 20.9 mJ m^{-2}, again significantly higher than our value. Tegze[104] has proposed a theoretical basis for Turnbull's empirical relation and his model predicts a value of 28 mJ m^{-2} for σ_{sl} at 230 K. These

Table 5-7. Changes of surface tension versus temperature (T) or mean size of clusters diameter (D)

T K	Diameter nm	Exp. J $m^{-3} s^{-1}$	Cal. J $m^{-3} s^{-1}$	sigma mJ m^{-2}	changes %
220	10	3.7E+30	3.2E+30	11.8	10.3
230	10	3.7E+30	3.2E+30	10.7	0.0
240	10	3.7E+30	3.3E+30	9.4	-12.1
230	2	1.4E+33	1.8E+33	9.2	-14.0
230	5	3.0E+31	3.3E+31	10.2	-4.7
230	10	3.7E+30	3.2E+30	10.7	0.0
230	20	4.6E+29	4.3E+29	11.1	3.7
230	50	3.0E+28	2.7E+28	11.6	8.4

values predicted by these relations are close to those measured for other molecules in our lab, so the discrepancy in the case of benzene is puzzling. It must be recalled however that our σ_{sl} is only a lower limit.

Finally, it is interesting to compare our σ_{sl} value of 11.7 mJ m^{-2} with the liquid surface tension σ_{lv} at the same supercooled freezing temperature. No experimental data is available at 230 K, but we can extrapolate existing room temperature data[57,105] to this supercooled freezing temperature. This gives a value of σ_{lv} = 35.4 mJ m^{-2}. This value is much higher than our solid-liquid value of 11.7 mJ m^{-2} because the difference of properties between liquid and vapor is much bigger than that between solid and liquid. Using these two values and Young's relation, $\sigma_{sl} = \sigma_{sv} - \sigma_{lv}$, we obtain a value of 47.1 mJ m^{-2} for σ_{sv}, the surface free energy of solid.

Very few values of σ_{sl} are available in the literature for other molecules. Table 5-8 summarizes most of the values from published literature. The number of molecules on the list is very small compared to the huge amount of molecules in the world. This demonstrates the difficulties to determine σ_{sl} value by any other methods.

By spraying small liquid drops into a cold cloud chamber and using Rayleigh scattering to monitor the onset of freezing, Stavely studied over a dozen of molecules and deduced their σ_{sl} values. Stavely's values should be considered as an upper limit as discussed in section 5.5.7. With a supersonic jet and by monitoring the rate of freezing with high resolution stimulated Raman spectroscopy (SRS), a value of 3.2 mJ m^{-2} was deduced for nitrogen at nucleation temperatures around 34 to 44 K.[13] Minarik[28] derived a σ_{sl} value of 10.1 mJ m^{-2} for acetylene clusters freezing at 155 K with CARS. By using a supersonic jet and monitoring the phase transition with electron diffraction, Bartell derived values of 4.7 mJ m^{-2} for CH_3CCl_3 at nucleation temperature of 165 K, 4.8 mJ m^{-2} for CCl_4 at 175 K, and 23 mJ m^{-2} for NH_3 at 128 K. If we compare the last two σ_{sl} values from Bartell's free jet expansion with Stavely's cloud chamber method, both are considerable lower than Stavely's values. This is in agreement with our value for benzene compared to Stavely's value. As we just mentioned earlier in this section, Stavely's value is an upper limit, our value is a lower limit. The true value of σ_{sl} must fall in between these two limits. Examining Table 5-8, we see that the molecules with hydro-bonding have the relative larger σ_{sl} values, such as water and ammonia. The molecules with relative small σ_{sl} values are nitrogen and CCl_4. More data from different

Table 5-8. σ_{sl} Values from different methods

		Cloud chamber			Free jet			
		Rayleigh Scattering			e. Diffraction		CARS	
Molecule	T_m K	T_L K	sigma mJ m^{-2}	Turnbull mJ m^{-2}	T_L K	sigma mJ m^{-2}	T_L K	sigma mJ m^{-2}
CH_3Cl	175.6	120	21.4	17.6				
H_20	273.2	232	30.8	32.9				
Naphthalene	353.1	258	30.1	31.1				
CH_2BrCH_2Br	282.7	216	21.0	20.4				
CBr_4	363.3	281	10.7	10.1				
$C_6H_5CO_2H$	395.0	275	34.8	30.9				
Diphenyl	344.0	285	24.0	24.8				
P_4 (white)	317.5	202	12.6	5.9				
CCl_4	**250.2**	**200**	**6.7**	6.7	**175**	**4.8**		
NH_3	**195.5**	**155**	**29.1**	28.2	**128**	**23.0**		
CH_3CCl_3	243.1				165	4.7		
C_6H_6	**278.4**	**208**	**20.4**	20.9			**230**	**11.7**
C_2H_2	192.7						155	10.1
N_2	63.2						34	3.2

molecules are needed to draw any broader conclusions about the correlation between molecular structure and σ_{sl} values.

5.6. Summary

Liquid benzene clusters of more than 1000 units were produced in a free jet expansion and found to begin freezing when experimental conditions made the clusters supercool to a temperature of about 230 K. A subtle indication for the nucleation of

freezing was employed in which the latent heat of fusion was detected by means of a temperature dependent peak shift. The duration of the phase transition of nucleation of freezing is believed to be about 0.4 μs, which is much less than previously speculated 100 μs.[88] The results yield a value of 11.7 mJ m^{-2} for the solid-liquid interfacial tension of benzene at 230 K. The experiments demonstrate that, as long as the difference in Raman shift of solid at the melting point T_m and liquid at a supercooled freezing temperature T_L is larger than the uncertainty in the CARS measurement (less than 0.05 cm^{-1} in our system), CARS can be used to detect the onset of freezing for a cluster. Thus the choice of molecules that can be studied with CARS is greatly increased.

BIBLIOGRAPHY

[1] Mcbride, J. M. Science **256,** 814, (1993)

[2] Gibbs, J. W. Trans. Conn. Acad. Arts Sci. II 382, (1876). ibid, II 343, (1878)

[3] John F. Ogilvie private communication, February, (1998)

[4] G. R. Wood and A. G. Walton, J. Appl. Phys., **41**, (7), 3027-36, (1970)

[5] V. K. Kumikov and Kh. B. Khokonov, J. Appl. Phys. **54** (3), 1346-50, (1983)

[6] Theoodore S. Dibble and Lawrence S. Bartell, J. Phys. Chem. **96**, 2317-22, (1992)

[7] Peter P. Wegener, J. Phys. Chem., **91**, 2479-81, (1987)

[8] Georg Koppenwallner and Carl Dankert, J. Phys. Chem., **91**, 2482-6, (1987)

[9] David Turnbull, J. Chem. Phys., **20** (2), 411-24, (1952)

[10] D. G. Thomas and L. A. Staveley, J. Am. Chem. Soc., **28**, 4569-77, (1952)

[11] Edward J. Valente and Lawrence S. Bartell, J. chem. Phys., **80** (4), 1451-7, (1984)

[12] Lawrence S. Bartell, Leo R. Sharkey, and Xianqian Shi, J. Am. Chem. Soc., **110** (21),7006-13, (1988)

[13] Rainer D. Beck, Max F. Hineman, and Joseph W. Nibler, J. Chem. Phys., **92** (12), 7068-78, (1990)

[14] Kyung Hee Lee, Nancy E. Triggs, and Joseph W. Nibler, J. Phys. Chem., **98**, 4382-8, (1994)

[15] Lawrence S. Bartell and Shimin Xu, J. Phys. Chem., **99**, 10446-53, (1995)

[16] Lawrence Bartell, J. Phys. Chem. **99**, 1080-9, (1995)

[17] L. S. Bartell, L. Harsanyi, T. S. Dibble, and P. J. Lennon, **94**, 60009-12, (1990)

[18] Lawrence S. Bartell, Laszlo Harsanyi, and Edward J. Valente, J. Phys. Chem. **93**, 6201-5, (1989)

[19] Jinfan Huang and Lawrence S. Bartell, J. Phys. Chem. **98**, 4543-50, (1994)

[20] C. A. Swenson and W. B. Person, J. Chem. Phys., **31**, (5), 1324-28, (1959)

[21] K. Liu, J. D. Cruzan and R. J. Saykally, Science, **271**, 929-33, (Feb., 1996)

[22] L. Colombo, D. Kirin, V. Volvosek, N. E. Lindsay, J. F. Sullivan, and J. R. Durig, J. Phys. Chem., **93**, (17), 6290-6, (1989)

[23] Patrick R. R. Langridge-Smith, Donard V. Brumbaugh, Christopher A. Haynam, and Donald H. Levy, J. Phys. Chem. **85**, (25), 3742-6, (1981)

[24] K. Yamanouchi, M. Okunishi, Y. Endo and S. Tsuchiya, J. Mol. Structure, **352/253**, 541-559, (1995)

[25] B. L. Chadwick, A. P. Milece, and B. J. Orr, Can. J. Phys., **72**, 939-53, (1994)

[26] Xiuling Li and Robert L. Whetten, Z. Phys. **D 26**, 198-200, (1993)

[27] Hans Dieter Barth and Friedrich Huisken, J. Chem. Phys., **78**, (5), 2549-59, (1987)

[28] Phil Minarik, Ph. D Thesis, OSU, (1996)

[29] H. Bonadeo, M. P. Marzocchi, E. Castellucci, and S. Califano, J. Chem. Phys., **57**, (10), 4299-303, (1972)

[30] Jeffrey H. Williams and Maurizio Becucci, Chem. Phys. **177**, 191-202, (1993)

[31] Renato Torre, Roberto Righini, Leonardo Angeloni and Salvatore Califano, J. Chem.Phys., **93**, (5), 2967-73, (1990)

[32] L. S. Bartell and T. S. Dibble, J. Phys. Chem. , **95**, 31159-66, (1991)

[33] Robert A. Alberty, "Physical Chemistry" 7th ed., John Wiley & Sons, (1987)

[34] G. E. Duvall, Rev. of Modern Physics, P523-79, (1977)

[35] Kazuyuki Tohji and Yoshitada Murata, Japanese J. Appl. Phys., **21**, (8), 1199-1204, (1982)

[36] A. Fruhling, Ann. Phys. Paris **6**, 401-480, (1951)

[37] M. Ghelfeengstein and H. Szwarc, Mol. Cryst. Liq. Cryst. **14**,273, (1971)

[38] M. Ghelfeengstein and H. Szwarc, Chem. Phys. Lett. **32**, 93, (1975)

[39] P. Pruzan, D. H. Liebenberg, and R. L. Mills, J. Phys. Chem. Solids **47**, 949, (1986)

[40] C. J. Craven, P. D. Hatton, C. J. Howard and G. S. Pawley, J. Chem. Phys., **98**, 108236-43, (1993)

[41] E. R. Anderson and R. G. Eades, Proc. Royal Soc. London, **218**, 537-52, (1953)

[42] A. J. Stace, D. M. Bernard, J. J. Crooks, and K. L. Reid, Molecular Physics, **60**, (3), 671-9, (1987)

[43] D. W. J. Cruickshank and J. A. S. Smith, Proc. R. Soc. London Ser. **A 247**, 1, (1958)

[44] G. E. Bacon, N. A. Curry and S. A. Wilson, Proc. R. Soc. London Ser **A 279**, 98, (1964)

[45] David Turnbell and Robert L. Cormia, J. Chem. Phys., **34**, (3), 820-31, (1961)

[46] See W. J. Dunning in " Nucleation", edited by A. C. Zettlemoyer, Marcel dekker, New York, (1969).

[47] James E. McDonald, Am. J. Phys., **30**, 870-77, (1962)

[48] James E. McDonald, Am. J. Phys., **31**, 31-41, (1963)

[49] Turnbell, D.; Fisher, J. C., J. Chem. Phys. **17**, 71, (1949)

[50] Theodore S. Dibble and Lawrence S. Bartell, J. Phys. Chem., **96**, 8603-10, (1992)

[51] Hockney, R. W., Eastwood, J. W., "Computer Simulations Using Particles", McGraw-Hill: New York, (1981)

[52] Jorgensen, W. L., J. Am. Chem. Soc., 103,335,341,345, (1981)

[53] Peter Harrrwell and David W. Oxtoby, J. Chem. Phys. **80**, (4), 1639-46, (1984)

[54] Grigory Natanson, Francois Amar, and R. Stephen Berry, J. Chem. Phys., **78**, (1), 399-408, (1983)

[55] R. H. Doremus, "Rates of Phase transformations", Academic Press, Orlando, (1985)

[56] A. Boni, "Physical Properties of Molecular Crystals, Liquids, and glasses", John Wiley & Sons, (1968)

[57] "Handbook of Chem. and Phys. 50th Ed.",. Chemical Rubber Co., (1969-70)

[58] J. Timmermans, "Physico-chemical constants of pure organic compound", Elsevier Publishinh Co., Inc, (1950)

[59] Carl. L. Yaws, <<Physical Properties>>, McGraw-Hill Publishing Co. Inc, (1977)

[60] J. W. Nibler and G. V. Knighten, "Coherent Anti-Stokes Raman Spectroscopy" in <<Raman Spectroscopy of gases and liquid ------ Current topics in Physics>>, (1979)

[61] Joseph W. Nibler and George A. Pubanz, "Coherent Raman Spectroscopy of Gases" in <<Advances in Non-linear Spectroscopy>> edited by R. J. Clark and R. E. Hester, John Wiley & Sons Lid. (1988)

[62] Ming Yang, Ph.D Thesis, OSU, (1990)

[63] Atlas Des molecules diatomiques, Laboratorie Aime Cotton Campus d'Orsay-Batimore 505, 91405 Orsay Cedex- France.

[64] Alan D. Richardson, M.S. Thesis, OSU, (1993)

[65] Peter V. Hobbs, <<Ice Physics>>, Clarendon Press Oxford, (1974)

[66] M. M. Thiery and J. M. Leger, J. Chem. Phys., **89**, (7), 4255-71, (1988)

[67] Kazuyuki Tohji and Yoshitada Murata, Japanese J. of Appl. Phys., **21**, (8), 1199-1204, (1982)

[68] M. Ito and T. Shigeoka, Spectrochimica Acta, **22**, 1029-44, (1966)

[69] M. Ghelfenstein and H. Szwarc, Molecular Crystals and Liquid Crystals, **14**, 273-81, (1971)

[70] T. J. Trout, S. Velsko, R. Bozio, P. L. Decola and R. M. Hochstrasser, J. Chem. Phys., **81**, (11), 4746-59, (1984)

[71] M. Ghelfenstein and H. Szwarc, Molecular Crystals and Liquid Crystals, **14**, 273-81, (1971)

[72] W. J. Dunning, "IR & Raman Studies of Molecular Motion in Plastic Crystals", in "The Plastically Crystalline State (Orientationally-Disordered Crystals) Ed by John N. Sherwood., John Wiley & Sons, (1979).

[73] Swenson, C. A., Person, W. B. Dows, D. A., and Hexter, R. M., J. Chem. Phys., **31**, 1324, (1959)

[74] G. Herzberg "Molecular Spectroscopy and Molecular Structure : Infrared and Raman Spectra of Polyatomic Molecules", Van Nostrand: Princeton, (1945)

[75] R.T. Bailey "IR & Raman Studies of Molecular Motion in Plastic Crystals" in "The Plastically Crystalline State (Orientationally-Disordered Crystals) Ed by John N. Sherwood., John Wiley & Sons, (1979).

[76] G. Pangilina, G. Guelachvili, R. Sooryakumar, and K. Narahari Rao, Phys. Rev. **B 39**, 2522 (1989)

[77] John F. Ogilvie, J. Chin. Chem. Soc., Invited pare "Mesophase I", **36**, 375-388, (1989)

[78] John F. Ogilvie, J. Chin. Chem. Soc., Invited paper "Meso phase II", **36**, 501-13, (1989)

[79] G. Del Mistro and A. J. Stace, Chem. Phys. Lett., **171**, (4), 381-4, (1990)

[80] Mee Y. Hahn and Robert L. Whetten, Phys. Rev. Lett., **61**, (10), 1190-3, (1988)

[81] David R. Miller, "Free jet Sources" in << Atomic and Molecular Beam Methods>> Vol **1**, edited by Giacinto Scoles, Oxford University Press, (1988)

[82] A. B. Hollinger and H. L. Welsh, Can. J. Phys. **56**, 974-82, (1978)

[83] David C. Easter, M. S. El-Shall, M. Y. Hahn and R. L. Whetten, Chem. Phys. Lett., **157** (4) 277-82, (1989)

[84] Richard K. Heenam, Edward J. Valente and Lawrence S. Bartell, J. Chem. Phys., **78**, (1), 243-8, (1983)

[85] Lawrence S. Bartell, Chemical Reviews, **86**, (3), 491-505, June, (1986)

[86] Per Linse, J. Am. Chem. Soc. **106**, 5425-30, (1984)

[87] Frederic J. Dulles and Lawrence S. Bartell, J. Phys. Chem. **99**, 17100-06, (1995)

[88] Lawrence S. Bartell and Frederic J. Dulles, J. Phys. Chem., **99**, 17107-12, (1995)

[89] Lawrence S. Bartell, Leo R. Sharkey, and Xianqian Shi, J. Am. Chem. Soc. **110**, (21), 7006-13, (1988)

[90] David C. Easter, A. P. Baronavski, and Michael Hawley, J. Chem. Phys., **78**, (1), 243-8, (1983)

[91] S. G. Lipsett, F. M. Johnson, and O. Mass, J. Am. Chem. Soc. **49**, 925, (1927)

[92] M. L. Dundon, J. Am. Chem. Soc. **45**, 2658, (1923)

[93] E. W. Muller, Z. Phys. **106**, 541, (1937)

[94] J. Sawai and M. Nishida, Z. Anorg. Allgen. Chem. **190**, 375, (1930)

[95] G. Tammah and W. Bochme, Ann. Phys. **12**, 820, (1932)

[96] M. A. Mauyrakh, A. S. Orlov, and M. R. Besshapova, Adgez. Raslavov (Naukova dumka, Kiev, USSR,1974), p. 103.

[97] S. N. Zadumkin, Kh. B. Khokonov, and J. G. Shebzukhova, Avtorshkoe svidetelstvo N4408198 (USSR), (1973).

[98] George E. Ewring and De T. Sheng, J. Phys. Chem., **92**, 4063-66, (1988)

[99] Steve Mayer, Ph. D Thesis, OSU, (1997)

[100] M. H. Schartz and R. P. Andres, J. Aerosol. Sci., **7**, 281-96, (1976)

[101] D. A. Jackson and B. Simic-Glavaski, Mol. Phys. **18**, (3), 393-400, (1970)

[102] M. Kappes and S. Leutwyler, "Molecular Beams of Clusters" in << Atomic and Molecular Beam Methods>> Vol **1**, edited by Giacinto Scoles, Oxford University Press, (1988)

[103] CRC chemistry and physical handbook, 77th, (1997)

[104] L. Gránásy, M. Tegze, and A. Ludwig, Mat. Sci. & Eng., **A133**, 577, (1991)

[105] CRC chemistry and physical handbook, 78th, (1998)